PROBABILISTIC SEISMIC HAZARD ASSESSMENT FOR THE FORGE SITE

University of Utah
Salt Lake City, Utah

Prepared for:

University of Utah
Salt Lake City, UT

Prepared by:

Wood Environment & Infrastructure Solutions, Inc.
180 Grand Avenue, Suite 1100
Oakland, California 94612

May 2020

Project No. 8619192750.04

TABLE OF CONTENTS

wood.

TABLES

FIGURES

PROBABILISTIC SEISMIC HAZARD ASSESSMENT FOR THE FORGE SITE

University of Utah
Salt Lake City, Utah

EXECUTIVE SUMMARY

This report presents an update of the probabilistic seismic hazard assessment (PSHA) conducted by Amec Foster Wheeler (2018) to obtain the mean annual frequency that specified levels of ground motion will be exceeded at four locations in the vicinity of the proposed FORGE (Frontier Observatory for Research in Geothermal Energy) site. The target sites are the FORGE drilling center, the town of Milford, UT, a central location in the adjacent windmills, and the Blundell geothermal plant.

The site lies within the Basin and Range province of North America, in an area characterized by the presence of numerous normal faults capable of generating large magnitude earthquakes. Most notably, the site is approximately 120 km from the closest segment of the Wasatch fault. The distribution of earthquakes in Utah is concentrated in the central part of the State, along the Wasatch range. Most of the earthquakes are small magnitude events, however the most recent estimate by the Working Group on Utah Earthquake Probabilities (WGUEP) is a probability of 43 percent that an earthquake with **M** ≥ 6.75 associated with ruptures along the Wasatch fault will occur in the next 50 years (WGUEP, 2016).

The main components of the PSHA are seismic source characterization and ground-motion characterization. The PSHA developed for FORGE specifically incorporated uncertainties in the models and model parameters that make up the seismic source and ground-motion characterization.

Seismic source characterization provides a probabilistic model for the rate of occurrence, spatial distribution, and size distribution of earthquakes within the region surrounding the site. Two types of seismic sources were included in the model: areal source zones, which are used to model the occurrence of distributed seismicity throughout the region; and local and regional faults, which are used to model the localized occurrence of larger magnitude earthquakes on mapped geologic features. The distributed seismicity source zones were developed based on

interpretations of the regional geology, seismicity, and tectonics. Local and regional faults are characterized based on geological investigations conducted by the University of Utah (local faults) and using the Quaternary faults database compiled by USGS.

The PSHA was conducted using the ground motion predictive equations (GMPEs) developed in the NGA-West 2 Project (Bozorgnia et al., 2014). These models provide the necessary characterization of ground motions for the local site conditions encountered at the four sites analyzed in this study.

Several updates are included in this report. First, the location of the FORGE drilling center has been re-assigned to be the centroid of the area that will be stimulated. This location is approximately 500 m from the FORGE drilling center used in the 2018 calculations. Second, since the publication of the 2018 PSHA report, the University of Utah has collected site velocity data that allowed for a re-evaluation of the Vs30 and basin-depth parameters necessary to adjust the NGA-West 2 ground motion models to the site conditions at each site. Third, based on new research conducted on segments of the Wasatch fault and on the Negromag fault, changes were made to the earthquake recurrence model of each fault. The effect of these changes was found to be generally very small. In addition to these updates, the effect of adding 1.3 more years of observed seismicity to the earthquake catalog developed by Amec Foster Wheeler (2018) was evaluated by statistical testing. The test results indicated that there was no need to update the recurrence model of the zones based on the additional observed seismicity.

While updating the hazard calculations, an error was discovered in the earthquake recurrence parameters used for the source zones in the Amec Foster Wheeler (2018) PSHA. This report presents corrected results and supersedes Amec Foster Wheeler (2018). The corrected results are significantly lower than the 2018 PSHA results. The results of the PSHA indicate that for short return periods the high-frequency hazard is controlled by small nearby earthquakes associated with the host distributed seismicity zone (the Basin and Range zone), while the low-frequency hazard is affected by larger magnitude, more distant earthquakes, such as those occurring on the nearest segment of the Wasatch fault. For long return periods, the hazard is dominated by earthquakes occurring on the local faults. The hazard at the FORGE drilling center, Milford, and Blundell Geothermal Plant is comparable, while the hazard at the windmills is relatively lower, due to its greater distance from the local faults and from the Intermountain Seismic Belt.

PROBABILISTIC SEISMIC HAZARD ASSESSMENT FOR THE FORGE SITE

University of Utah
Salt Lake City, Utah

1.0 INTRODUCTION

This probabilistic seismic hazard assessment (PSHA) was performed to obtain the mean annual frequency that specified levels of ground motion will be exceeded at four locations near the proposed Frontier Observatory for Research in Geothermal Energy (FORGE) site in central Utah. The target sites are the FORGE drilling center, the town of Milford, UT, a central location in the adjacent windmills (referred to in the following as windmills), and the Blundell geothermal plant. Table 1-1 lists the coordinates of the four sites, which are shown in Figure 1-1. The location of the FORGE drilling center shown in Table 1-1 and Figure 1-1 is approximately 500 m away from the location of the FORGE drilling center used in Amec Foster Wheeler (2018). This location represents the possible centroid of the area that will be stimulated (Kris Pankow, email communication on April 10, 2020).

1.1 OBJECTIVES

The scope of work for this study involved developing a seismic hazard model that encompasses the region within approximately 300 km of the FORGE site. Due to attenuation of seismic wave with distances in the western US, earthquakes occurring at greater distances are not expected to contribute to the site hazard. The model includes regional and local earthquake sources, each characterized in terms of the recurrence rate of earthquakes as a function of magnitude. The sources were developed and characterized based on the observed seismicity and geologic data. A suite of ground motion prediction equations (GMPEs) applicable to Utah were selected for use to assess the ground motions that local and regional earthquakes may produce at the sites.

The project scope of work consisted of three tasks: 1) develop a seismic source characterization model; 2) select GMPEs appropriate for the tectonic characteristics of the earthquake sources and the local site conditions; and 3) calculate PSHA at the four locations. The hazard analysis was conducted using a probabilistic approach. Seismic hazard results are presented for peak ground acceleration and 5% damped response spectra ordinates for spectral periods of 0.02,

0.05, 0.075, 0.10, 0.20, 0.50, 1.0, 2.0, and 5.0 sec (frequencies of 50, 20, 13.3, 10, 5, 2, 1, 0.5 and 0.2 Hz). The hazard is computed for a broad period range in order to provide a more complete description of the site hazard and to provide results that can be used in analyses of various types of structures.

Following the publication of Amec Foster Wheeler (2018) PSHA report, Wood was retained to conduct a series of analysis to evaluate the need to update the FORGE Probabilistic Seismic Hazard model based on new information. Specifically, the Department of Energy (DOE) has indicated that the seismic hazard model should be updated based on 1) new information on the regional setting and structure; and 2) new data pertaining the velocity model at the site. This report and the results of the PSHA analyses presented herein include the new information that was evaluated. During these evaluations, an error was discovered in the 2018 Amec Foster Wheeler calculations. The hazard results presented in this report are obtained with the correct parameters and therefore supersede the 2018 PSHA presented in Amec Foster Wheeler (2018). The corrected results are significantly lower than the 2018 PSHA results for all sites.

1.2 DOCUMENT STRUCTURE

This report is organized into five parts:

Section 1 – Introduction

This section presents the objectives of the study and describes the document structure.

Section 2 – Earthquake Catalog

This section describes the compilation and analysis the earthquake catalog for the project region used in the development of the SSC model and its update.

Section 3 – Seismic Hazard Model

This section describes the seismic hazard model developed for the FORGE region and its update.

Section 4 – Probabilistic Seismic Hazard Analysis

This section describes the results of the PSHA conducted for the four sites of interest and the development of ground-motion response spectra.

Section 5– Conclusions

This section presents the study conclusions, based on the seismic hazard results at the four localities of interest.

2.0 EARTHQUAKE CATALOG

The primary source for the compilation of the earthquake catalog is the catalog of earthquakes for the "Utah Region" (lat. 36.75° to 42.50° N, long. 108.75° to 114.25° W) from 1850 through 2016, compiled by Arabasz et al. (2017). This compilation is termed the "Utah catalog" in the following. The catalog contains mostly "Best-Estimate Magnitudes", BEM in the following, which is either an observed moment magnitude **M**, value of **M** obtained by conversion using another magnitude type, or a magnitude assumed equivalent to **M** (Arabasz et al., 2016).

The spatial extension of the Utah catalog is not sufficient to cover the region of interest for the source characterization. The project catalog was expanded to the south and to the west by adding records from the catalog used in the National Seismic Hazard Map project of 2014 (Petersen et al., 2014). Six different catalogs were downloaded from the USGS website (https://github.com/usgs/nshmp-haz-catalogs). Three catalogs cover the Central and Eastern U.S. (CEUS) and three catalogs cover the Western U.S. (WUS). In the study region, the separation between CEUS and WUS catalog occurs at approximately longitude 113.8° W. Figure 2-1 reproduces a table from the USGS website that describes the characteristics of the six catalogs. The top three rows refer to the CEUS catalogs, the bottom three to the WUS catalogs. The three catalogs are described here for CEUS since it is the same for WUS. In all catalogs duplicated and non-tectonic events caused by mining and explosions have been removed. Catalog *c2 contains both dependent earthquakes (aftershocks and foreshocks) and events possibly related to fluid injection (PFI); catalog *.c3 does not contain dependent events but contains PFI; catalog *.c4 does not contain dependent events nor PFI. For the purpose of this study, we need to maintain dependent events in the catalog, but we need to remove PFI, therefore we have first compared catalogs *.c3 and *c4 to identify PFI, then removed the PFI from *.c2. The corrected CEUS and WUS *.c2 catalogs were merged, sorted in chronological order, and trimmed to the study region. This catalog is termed "NSHM catalog" in the following.

Two important issues need to be resolved for using the NSHM catalog: 1) the catalog only extends to the end of 2012; 2) the uniform moment magnitude is E[M] (EPRI/DOE/NRC, 2012)

not BEM. The first issue is addressed by truncating the completeness of the NSHM catalog to the end of 2012 (see Section 3.3). The second issue is addressed in Section 2.1.

2.1 NSHM MAGNITUDES AND UTAH MAGNITUDES

Figure 2-2 shows the 2,129 earthquakes common to the Utah and NSHM catalog. For these earthquakes, we have compared the moment magnitude from the Utah catalog with the expected moment magnitude (E[**M**]) from the NSHM catalog (Figure 2-3). The plot on the left-hand side of Figure 2-3 shows the differences between NSHM E[**M**] and Utah Catalog BEM versus magnitude, while the plot on the right-hand side of Figure 2-3 shows the differences versus time. While the plots indicate a linear trend, they also show a wide dispersion of the data, which is greater for larger magnitudes and older events.

Using both catalogs, we collected the seismicity within an area of 50-km radius from the center of the FORGE site. For this analysis we assumed that the equivalent earthquake counts for the Utah catalogs are equal to 1 for each earthquake. We used the completeness time intervals from Arabasz et al. (2016) for the Utah region, and Mmax of 6.75 (Arabasz et al., 2016) for the recurrence calculations done using the Utah catalog, and Mmax of 8 (Petersen et al., 2014) for the recurrence calculations done using the NSHM catalog. Both catalogs are declustered using the method by Gardner and Knopoff (1974). It was noticed that the earthquake of November 14, 1901 (BEM 6.63, E[**M**] 6.5) has different epicentral coordinates in the Utah and NSHM catalogs, such that it falls inside the 50-km radius area in the Utah catalog, but not in NSHM. To be able to compare the recurrence from the two seismicity models, the earthquake was considered either inside the 50-km area for both catalogs, or outside for both catalogs. Figure 2-4 shows the comparison between the mean and fractile earthquake frequency distribution obtained from the Utah catalog (green) and the corresponding distributions obtained from the NSHM. The plot on the left-hand side of Figure 2-4 shows the recurrence comparisons assuming that the coordinates of the 1901/11/14 earthquake are as in the Utah catalog (i.e., the earthquake is inside the 50-km area); the plot on the right-hand side of Figure 2-4 shows the case where the coordinates of the 1901/11/14 earthquake are as in NSHM (i.e., the earthquake is outside the 50-km area). While the slope of the recurrence curves is slightly steeper for Utah, the difference is small enough that the two catalogs can be considered equivalent. Based on this comparison, and solely for the scope of this study, NSHM E[**M**] are used as is to extend the Utah catalog to the south and to the west to cover the study region.

2.2 CATALOG DECLUSTERING

The PSHA formulation developed by Cornell (1968, 1971) assumes that the occurrence of earthquakes is a Poisson process. Studies such as Gardner and Knopoff (1974) have shown that when foreshocks and aftershocks (dependent events) are removed from an earthquake catalog, the remaining (independent) events can be considered to conform to a Poisson process in time.

Dependent events have been removed from the updated earthquake catalog using multiple approaches. The criteria applied for this study are those of Grünthal (1985, updated by pers. comm., 2002), Gardner and Knopoff (1974), Uhrhammer (1986), and EPRI/SOG (1988). The EPRI/SOG (1988) model was originally developed by Veneziano and Van Dyke (1985), although details of the methodology were only available in form of a draft report. As discussed in EPRI/DOE/NRC (2012), the advantages of the EPRI/SOG (1988) approach are that it is insensitive to incompleteness because a homogeneous Poisson process is only assumed in proximity to the earthquake sequence being tested and that it does not assume a priori a shape for the clusters.

The first three methods address the uncertainty in the duration and extent of the time and space windows used to identify dependent events, while the fourth method is conceptually different. All together the four declustering algorithms address epistemic uncertainty in the identification of dependent events.

The results of the declustering are summarized in Table 2-1: the initial catalog contains 32,763 earthquakes, the declustered catalogs vary considerably in the overall number of earthquakes, with the larger differences observed in the smaller magnitude intervals.

2.3 ANALYSIS OF CATALOG COMPLETENESS

Arabasz et al. (2017) conducted an in-depth analysis of completeness for the region covered by the project catalog. Their estimates of completeness for the Utah Region (UTR) are used in this project without modification. The portion of the study region that falls within the WGUEP region uses the completeness interval obtained for that project (WGUEP, 2016). For the portion of the study area covered by the NSHM catalog, the completeness intervals for the UTR were applied, but time elapsed was calculated based on a catalog ending in 2012. The start of the completeness period for various magnitude intervals for UTR and WGUEP is shown in Table 2--2.

2.4 EVALUATE THE NEED TO UPDATE THE EARTHQUAKE CATALOG BASED ON RECENT OBSERVED SEISMICITY

In PSHA the earthquake catalog is used primarily to develop earthquake frequency relations for zones of distributed seismicity and to develop models that represent the spatial distribution of the seismicity within the zones. Observed seismicity is also used to guide the selection of appropriate maximum magnitude and focal depth distributions for source zones.

The latest available update of the earthquake catalog for the Utah region (Arabasz et al., 2017), includes updates and revisions to the historical seismicity prior to 1962 (Arabasz et al., 2019). The catalog used in NSHM14 was updated for the 2018 National Seismic Hazard Map (NSHM18 in the following, Petersen et al., 2019). It is important to note that the only the declustered catalog is available for download.

The FORGE catalog was compared to the NSHM18 catalog for the area and time period. All comparisons were made with the FORGE catalog declustered using the Gardner and Knopoff (1974) method. An initial comparison showed 36 events within the Utah region that were found in NSHM18 but not in FORGE. Using Arabasz et al. (2019) for the pre-1962 records, and notes by Dr. Arabasz (2020, written communication) for the remaining cases, all the discrepancies were reconciled.

The common events identified in the FORGE and NSHM18 catalog were compared in terms of location and magnitude. The location is generally consistent between the catalogs with a few outliers that appear caused by typos in the epicentral coordinates. The analysis of magnitudes shows that NSHM18 magnitude are generally lower than FORGE for small **M**, and higher for large **M**. When compared to the NSHM14, the magnitudes from NSHM18 are consistently higher.

The comparison between NSHM18 and FORGE catalogs identified 45 events from 2017 to April 9, 2018 that can be used to evaluate the need to update the FORGE model with regard to the prediction of future earthquakes within zones of distributed seismicity. The first observation is that the post-2016 seismicity is distributed where pre-2016 earthquakes have occurred; therefore, the pattern of observed seismicity does not suggest the need to update the spatial density distribution of seismicity. The second observation is that the largest events occurred

after 2016 are well within the maximum magnitude range for the source zone, indicating that there is no need to update the maximum magnitude distributions.

To evaluate the need to update the recurrence rates, a statistical test was used. Under the null hypothesis, the number of earthquakes observed in the time elapsed since the end of the FORGE catalog is consistent with the number of earthquakes predicted by the long-term earthquake rates obtained using the FORGE catalog. The FORGE seismic hazard model (Amec Foster Wheeler, 2018) uses the Poisson recurrence model for the distributed seismicity sources. Given the frequency of earthquakes (λ) and the time interval of observation (t), the probability of observing exactly n earthquakes is given by:

$$P[N = n] = \frac{(\lambda t)^n e^{-\lambda t}}{n!} \quad (2\text{-}1)$$

An exact Poisson test (e.g., Fay, 2010) was performed to test the null hypothesis that the observed number of earthquakes in the time elapsed between the end of the Amec Foster Wheeler (2018) catalog (i.e., 12/31/2016) to the end of the updated NSHM18 catalog (i.e., 4/9/2018) has been generated by a natural process with true rate of earthquakes equal to the long-term earthquake rate of the hazard model. The time interval is equal to 1.3 years (t in Equation 1). Because the interest is in evaluating whether the true rate should be higher, a one-sided test is used. The test is performed by calculating the probability of observing a number n of earthquakes with **M** ≥ 3.0, or greater counts, given the true rate λ_i, where λ_i is one member of the uncertainty distribution for λ calculated from the FORGE model parameters. The test is defined by the following equation:

$$P[N \geq n_{obs}|\lambda_i] = 1 - \sum_{n=0}^{n-n_{obs}-1} P[N \geq n|\lambda_i] \quad (2\text{-}2)$$

The equation is used to evaluate each term of the summation from n = 0 to n = $n_{obs\ -1}$. Probabilities smaller than 5% reject the null hypothesis (i.e., fail the test).

The mean rate (λ_i) of earthquakes with **M** ≥ 3 can be obtained from the recurrence curves developed for the FORGE study and is used to calculate the mean predicted number of earthquakes greater or equal than **M** 3 ($N \geq n|\lambda_i$), which is 11.87. During this time interval, the NSHM18 catalog shows 13 earthquakes (n_{obs}) with **M** greater or equal than 3 in zone BR (Basin and Range) and none in the other zones. From Equation 2, the probability is 77%. The process was repeated for **M** 3.55, resulting in a probability of 91% as shown in Table 2-3. In both cases,

the probability is greater than 5% indicating that the predicted rates and the recent observed seismicity are not inconsistent.

3.0 SEISMIC HAZARD MODEL

This section describes the seismic hazard model developed for FORGE.

A PSHA incorporates both aleatory uncertainty and epistemic uncertainty. Aleatory uncertainty (or variability) is the natural randomness in a process, and epistemic uncertainty is the scientific uncertainty in characterizing the process due to limited data and knowledge. Examples of aleatory uncertainty are variation in the peak ground motion of individual recordings about a median ground-motion relationship, and the location and magnitude of the next earthquake. Examples of epistemic uncertainty are alternative models for ground motion estimation, the estimated long-term rate of slip on a particular fault, and the statistical uncertainty in quantifying the recurrence rate of earthquakes from a finite set of earthquake data. In this project uncertainties are addressed using logic trees. Methodologies for quantifying epistemic uncertainty include the development and weighting of alternative interpretations of seismic source characteristics to provide a structured characterization of epistemic uncertainty suitable for seismic hazard computation (Budnitz et al., 1997). The weighted alternative interpretations can be expressed by the use a sequenced series of nodes and branches on a logic tree (e.g., Kulkarni et al., 1984; EPRI-SOG, 1988).

The following sections contain descriptions of the logic tree framework for the FORGE seismic hazard model; descriptions of the distributed seismicity source zones and of the local and regional faults; and a description of the ground motion predictive equations implemented in the seismic hazard analysis.

3.1 SEISMIC SOURCE CHARACTERIZATION MODEL

The seismic source characterization model includes two types of seismogenic sources: areal source zones that model distributed seismicity throughout the region (Section 3.1.1), and fault sources that act as localizers of larger magnitude earthquakes. The fault sources are further divided between local faults (Section 3.1.2), which are located within approximately 50 km of the site, and regional faults (Section 3.1.3), that are located at greater distances from the site. The characterization of the local faults was based information gathered as part of this study. The

characterization of the regional faults was based on the 2014 National Seismic Hazard Maps (NSHM) characterization developed by Petersen et al. (2014).

3.1.1 Areal Source Zones

The study area is covered by three areal source zones simplified from the zones from the NSHM (Petersen et al., 2014). Table 3-1 summarizes the characterization of the areal source zones, which are shown in Figure 3-1.

The spatial distribution of future earthquakes was modeled using kernel density estimation (e.g., Silverman, 1986). A Gaussian kernel was selected to model the spatial distribution. Selection of the kernel size parameter h controls the balance between accurately portraying the areas of high seismicity without introducing areas of unrealistically low seismicity in areas of sparse seismicity. This balance was achieved by using the adaptive kernel smoothing recommended by Stock and Smith (2002), in which the kernel size is adjusted throughout the study region, decreasing in size in areas of higher data (earthquake) density and increasing in size in areas of sparse data. The Stock and Smith (2002) adaptive kernel approach is similar in concept to the approach used by Petersen et al. (2014) in the NSHM. Adaptive kernel smoothing spatial density models were developed for each of the areal source zones using each of the four alternative declustered earthquake catalogs.

Earthquake recurrence rates for the areal source zones were modeled by a truncated exponential magnitude distribution with parameters determined using the maximum likelihood formulation of Weichart (1980). Epistemic uncertainty in the recurrence parameters was modeled by a joint distribution of earthquake rate and b-value calculated from the likelihood formulation. Twenty-five alternative pairs of earthquake rate and b-value were developed for each of the alternative maximum magnitudes listed in Table 3-1 and for each of the four alternative declustered earthquake catalogs.

The maximum magnitude distributions for the source zones developed by Petersen et al. (2014) were adopted for use in this study.

3.1.1.1 Rocky Mountain

The Rocky Mountain Areal Source Zone encompasses the northeast corner of the study area. The source area includes the north-south trending Rocky Mountain chain. The Rocky Mountains

are a result of uplift during the Laramide orogeny and have had relatively low rates of historical seismicity.

The strike distribution for earthquakes in this zone was assumed to be random. Based on the style of faulting of mapped faults and available focal mechanisms, future earthquakes are assumed to be an equal mix of normal and strike-slip earthquakes. The assigned dip aleatory distribution was 35 (0.2), 50 (0.6), and 65 (0.2) degrees for normal ruptures and 90 degrees for strike-slip ruptures. The maximum depth of seismogenic rupture for this zone could not be directly assessed from the seismicity due to the limited number of earthquakes. Therefore, the epistemic distribution is assessed to be 8 km (0.2), 12 km (0.6), and 16 km (0.2), consistent with results obtained from the analysis of the seismicity of the entire region.

3.1.1.2 Basin and Range

The Basin and Range Areal Source Zone encompasses the majority of the study area including the FORGE site. The Basin and Range is defined by approximately north-south trending extensional valleys and mountain ranges. Most faults in the source zone are basin bounding normal faults.

Strike distribution for this study was assumed to be N30E. Based on the style of faulting of mapped faults and available focal mechanisms, future earthquakes are modeled as a mixture of 70 percent normal faulting and 30 percent strike slip faulting. The assessed aleatory distribution for rupture dip was 35 (0.2), 50 (0.6), and 65 (0.2) degrees for normal ruptures and 90 degrees for strike-slip ruptures. The epistemic distribution for maximum depth of seismogenic rupture assessed from analysis of the seismicity is 8 km (0.2), 12 km (0.6), and 16 km (0.2).

3.1.1.3 Colorado Plateau

The Colorado Plateau Areal Source Zone encompasses the southeastern portion of the study area. The Colorado Plateau is relatively undeformed and unfaulted in comparison to the Basin and Range and Rocky Mountains.

Strike distribution for this study was assumed to be random. Based on the style of faulting of mapped faults and available focal mechanisms, future earthquakes are assumed to be an equal mix of normal and strike-slip earthquakes. The assumed aleatory dip distribution was 35 (0.2), 50 (0.6), and 65 (0.2) degrees for normal ruptures and 90 for strike-slip ruptures. The f distribution for maximum depth of seismogenic rupture for this zone could not be directly assessed from the

seismicity due to the limited number of earthquakes available. The epistemic distribution is assumed to be 8 km (0.2), 12 km (0.6), and 16 km (0.2), consistent with results obtained from the analysis of the seismicity of the entire region.

3.1.2 Local Faults

Three local faults within 50 km of the FORGE site were identified as potentially active (Figure 3-2 and Table 3-2). Because down dip geometry is poorly defined for these faults they are assigned an epistemic distribution for dip of 50 (0.6), 65 (0.2), and 35 (0.2) degrees. Earthquake recurrence for the faults was modeled using the Youngs and Coppersmith (1985) characteristic magnitude distribution. The characteristic magnitude is calculated from the rupture dimensions using alternative empirical models (Hanks and Bakun, 2008, Stirling et al., 2008; Wesnousky, 2008). The use of three alternative equations, combined with nine alternative rupture geometries (three dips x three seismogenic depths), creates an epistemic distribution for characteristic magnitude.

The age of deformation of the local faults is also poorly known. Based on the limited information gathered, they were assigned a common wide epistemic distribution for slip rate of 0.002 (0.125), 0.06 (0.75), and 0.2 (0.125) mm/yr.

3.1.2.1 Opal Mound

The Opal Mound fault runs northeast-southwest along the western flank of the Mineral Mountains for 7 km. It is an east-dipping normal fault with a surface trace defined by siliceous hydrothermal deposits. Along the trace of the fault there are discontinuous fault offsets of 5 to 33 cm in a 10-m wide zone. The surface expression of the fault may be mineralization due to hydrothermal fluids moving along the fault promoting differential erosion rather than tectonic movement on the fault (Kleber, 2017). The eastern dip into the range front is atypical for the Basin and Range province. Knudsen et al. (2019) concluded the most recent activity on the fault may be late Pleistocene in age.

3.1.2.2 Negromag Wash

The Negromag Wash fault strikes east-west for 10 km in the Mineral Mountains, dipping to the north. The geomorphic expression of the fault is an approximately 1 km long, 1 to 3 m scarp which offsets Pleistocene alluvial fans. Knudsen et al. (2019) completed a paleoseismological study of the region surrounding the FORGE site and concluded the Negromag Wash fault was most likely a pre-Quaternary feature. They conclude the fault scarp is the result of differential

erosion rather than movement on the fault. Based on the results of this study, the likelihood of activity of the Negromag fault was lowered to 0.4 from 1.0.

3.1.2.3 Mineral Mountain West

The Mineral Mountain West fault zone runs northeast-southwest along the western flank of the Mineral Mountains and into the basin. The northern 8 km of the fault zone contain a graben with a mean scarp height of 3.5 m on internal horst and graben blocks. The highest slip rates are in the middle of the fault zone. The fault zone is 38 km long with an assigned maximum rupture length of 15 km. Knudsen et al. (2019) concluded the most recent activity on the fault may be late Pleistocene in age.

3.1.3 Regional Faults

Within the study area 52 individual faults and fault segments were identified based on the National Seismic Hazard map (NSHM) source faults (Table 3-2 and Figure 3-3; Petersen et al., 2014). Faults used in the NSHM are more than 50 km from the study sites. Of these, the Kane Spring Wash fault is strike-slip and the remainder are normal faults. All of the faults are with in the Basin and Range Areal Source Zone and have epistemic uncertainties in dip of 50 (0.6), 65 (0.2), and 35 (0.2) degrees for the normal faults and 90 for the strike slip fault. Earthquake recurrence rates are assessed using the slip rate distributions listed in Table 3-2 and the Youngs and Coppersmith (1985) characteristic magnitude distribution. The characteristic magnitude is calculated from the rupture dimensions using alternative empirical models (Hanks and Bakun, 2008, Stirling et al., 2008; Wesnousky, 2008). The use of three alternative equations, combined with nine alternative rupture geometries (three dips x three focal depths), creates an epistemic uncertainty distribution for the characteristic magnitude.

The Wasatch fault zone is the longest and most active of the faults included and its SSC model is further discussed in section 3.1.3.1.

3.1.3.1 Wasatch

The Wasatch fault zone is an approximately 200 km long normal fault that bounds the western edge of the Wasatch Mountains. It stretches from north of the Idaho border to south of Provo, UT. Although the fault zone has not generated a large earthquake during the historical period, paleoseismic evidence suggests large earthquakes occur on the fault. The Wasatch fault zone is more than 120 km to the northeast of the study sites.

The characterization of the Wasatch fault zone is adopted from Petersen et al. (2014). The fault zone is divided into seven individual segments that can break individually or as one fault that stretches the entire length of the fault zone (Table 3-3). The Wasatch fault zone is modelled in three alternative ways: 1) an unsegmented fault, generating a 127-km long rupture anywhere along its entire length; 2) a set of seven individual segments, each rupturing its full length; 3) an unsegmented fault that can generate earthquakes ruptures with lengths of 20 (0.3), 30 (0.3), 40 (0.3) and 50 (0.1) km. The characteristic magnitude is calculated from the rupture dimensions using alternative empirical models (Hanks and Bakun, 2008; Stirling et al., 2008; Wesnousky, 2008). The use of three alternative equations, combined with nine alternative rupture geometries (three dips x three focal depths), creates a characteristic magnitude distribution.

Two of the segments of the Wasatch fault, the Provo and Nephi segments have new reported slip rates based on recent trenching studies (Bennet et al., 2018 and Duross et al., 2017, respectively). These studies both concluded the slip rate was lower than the rate used by Petersen et al. (2014) and the slip rate distributions for these segments were adjusted to incorporate these lower rates for the individual segment portion of the Wasatch fault model.

3.1.4 Evaluate the Need to Update the Seismic Source Model

A review of literature published since the Amec Foster Wheeler (2018) report was conducted to identify new data or models that could be used to update elements of the source characterization models. Table 3-4 lists the articles that were evaluated during this review and summarizes their potential effect on the source model. As indicated in the previous sections, recent information was used to modify the slip rate distribution and probability of activity assessment of faults.

3.2 GROUND MOTION CHARACTERIZATION MODELS

In PSHA earthquake ground motions are typically specified in terms of alternative ground-motion-prediction equations (GMPEs). There are two necessary components of a GMPE: 1) a relationship for the median amplitude (mean log amplitude) of ground motions as a function of earthquake magnitude, source-to-site distance, and spectral frequency of interest, and other variables as appropriate; 2) a relationship for the aleatory variability of the ground motion about the median amplitude. To address uncertainty in the GMPEs, four alternative GMPEs were selected for the 2018 FORGE seismic hazard model (Amec Foster Wheeler, 2018). These are four

of the NGA-West2 ground motion models: the Abrahamson et al. (2014); Boore et al. (2014); Campbell and Bozorgnia (2014); and Chiou and Youngs (2014). These are the GMPEs used in the NSHM for sites other than rock in the WUS (Petersen et al., 2014).

The four NGA West 2 GMPEs cover a wide spectral range and are defined for the ten spectral frequencies chosen for this analysis (see Section 1.1). The four models can be directly used to assess ground motions for site conditions specified in terms of VS30, the time-averaged shear wave velocity of the top 30 m. Figure 10 of Zhang et al. (2018) shows Vs profiles to a depth of 400 m for the FORGE drilling center and the town of Milford. Similar profiles were provided by Dr. Pankow (2020, written communication) for the center of the windmills and the Blundell plant. These profiles were used to obtain site-specific V_{S30}. The four NGA-West2 GMPEs also include parameterization for basin depth in terms of depth to a shear wave velocity of 1 km/s, $Z_{1.0}$, or depth to a shear wave velocity of 2.5 km/s, $Z_{2.5}$. Values of these parameters were obtained from the velocity profiles for each site and applied in the hazard calculations. Table 3-5 lists the V_{S30}, and parameters $Z_{1.0}$ and $Z_{2.5}$ obtained at each site.

A model for the epistemic uncertainty in median ground motions was developed by Al Atik and Youngs (2014) as part of the NGA-West2 project. The model provides values of the standard deviation in ln(median) motion as a function of magnitude and structural period. The epistemic uncertainty in the NGA-West2 median motions was represented in the GMC logic tree by the three-point discrete representation of a normal distribution developed by Keefer and Bodily (1983) in which the central estimate is given a weight of 0.63 and the 5th and 95th percentiles (located at ±1.645 sigma) are each given a weight of 0.185.

4.0 PROBABILISTIC SEISMIC HAZARD ANALYSIS

The development of design ground motions for the four locations near the proposed FORGE site involved performing a PSHA using the seismic sources and the ground-motion models described in Section 3.

The following sections illustrate the approach used to perform the analyses and the results of the PSHA for the reference site conditions.

4.1 PSHA Analysis Approach

The mathematical formulation used in most PSHAs assumes that the occurrence of damaging earthquakes can be represented as a Poisson process. Under this assumption, the probability that a ground-motion parameter, Z, will exceed a specified value, z, in time period t is given by (e.g. Cornell, 1968, 1971).

$$P(Z > z \mid t) = 1 - e^{-\nu(z)\cdot t} \le \nu(z)\cdot t \tag{4-1}$$

where ν(z) is the average frequency during time period t at which the level of ground-motion parameter Z exceeds value z at the site from all earthquakes occurring in all sources in the region. Equation (4-1) is valid provided that ν (z) is the appropriate average value for time period t. In this study, the hazard results are reported in terms of the frequency of exceedance ν(z).

The frequency of exceedance ν(z) is a function of the frequency of earthquake occurrence, the randomness of size and location of future earthquakes, and the randomness in the level of ground motion that future earthquakes may produce at the site. It is computed by the following expression:

$$\nu(z) = \sum_n \alpha_n(m^0) \int_{m^0}^{m^u} f(m) \left[\int_0^\infty f(r|m) \cdot P(Z > z|m,r) \cdot dr \right] \cdot dm \tag{4-2}$$

where $\alpha_n(m^0)$ is the frequency of earthquakes on source n above a minimum magnitude of engineering significance, m^0; f(m) is the probability density of earthquake size between m^0 and a maximum earthquake the source can produce, m^u; f(r|m) is the probability density function for distance to an earthquake of magnitude m occurring on source n; and P(Z>z|m,r) is the probability that, given an earthquake of magnitude m at distance r from the site, the peak ground motion will exceed level z. The frequency of earthquake occurrence, $\alpha_n(m^0)$, and the size distribution of earthquakes, f(m), were determined by the earthquake recurrence relationships. The distribution for the distance between the earthquake rupture and the site was determined by the geometry of the seismic sources. The conditional probability of exceedance, P(Z>z|m,r), was determined using the GMPEs described in Section 3.3. The GMPEs defined the level of

ground motion in terms of a lognormal distribution. Based on the studies presented in EPRI (2006), the ground-motion distributions were not truncated in the PSHA calculation.

The seismic hazard model for the site region described in Section 3 treats all the parameters of Equation (4-2) as uncertain and specifies discrete probability functions for each one. The result is a large number of alternative parameter sets, each with a finite probability that it represents the "correct" parameter set. The computation of $\nu(z)$ is made for a particular parameter set, and the result is assigned the probability associated with that parameter set. The process is repeated over all parameter sets, producing a discrete probability density for the frequency of exceedance, $\nu(z)$. The probability density for $\nu(z)$ is then used to compute the mean or expected hazard and various percentiles of the distribution that define the uncertainty in the hazard given the uncertainty in the input parameters.

Wood E&IS's in-house set of seismic hazard software was used to perform the PSHA calculations. The computational scheme used to compute the hazard involves replacing the integrals of Equation (4-2) with summations over 0.1-unit magnitude and small distance intervals (e.g., 0.1 km for distances less than 10 km, 1 km for distances less than 100 km). The distance density function, $f(r|m)$, was computed numerically over each source region (assuming either a uniform density or a spatially varying density computed using a Gaussian kernel density estimator), assuming that each earthquake has a finite rupture area dependent on magnitude with the orientation of ruptures specified as described in Table 3-1. The fault sources are modeled as planar features with magnitude-dependent rupture areas located equally likely along the length of each fault. The probability function $P(Z>z|m,r)$ was computed assuming that peak ground motions are lognormally distributed about the specified median predictions from the GMPEs.

The hazard was computed using a fixed lower-bound magnitude (m^0 in Equation [3-2]) of **M** 4.0. The distance density functions were computed consistent with the distance measure used in the GMPEs.

Distributions for the annual frequency of exceeding various levels of peak ground acceleration and 5% damped response spectra were computed for spectral periods of 0.02, 0.05, 0.07, 0.10, 0.20, 0.50, 1.0, 2.0, and 5.0 s (frequencies of 50, 20, 13.3, 10, 5, 2, 1, 0.5 and 0.2 Hz). At each ground-motion level, the complete set of results forms a discrete distribution for frequency of

exceedance, ν(z). The computed distributions were used to obtain the mean frequency of exceeding various levels of peak ground motion (mean hazard curve), as well as hazard curves representing various percentiles of the distributions. The logic trees represent a best judgment as to the uncertainty in defining the input parameters, and thus the computed distributions represent the implied confidence in the output, the estimated hazard.

4.2 EFFECT OF MODEL UPDATES ON PSHA

Figure 4-1 illustrates the effect of updating the slip rate of the Provo segment of the Wasatch fault, and the probability of activity of the Negromag fault. The Figure compares the hazard result at the FORGE drilling center for PGA, and spectral acceleration for periods of 0.2 s and 1 s. These changes produce a small reduction in seismic hazard because the slip rate and the probability of activity were lowered.

Similarly, Figure 4-2 shows the effect of using the updated site characterization parameters for the FORGE drilling center. This site is chosen as an example because it shows the largest difference in V_{S30} between 2018 PSHA and the update. Results vary depending on the site, but in general show small variations of the mean hazard.

4.3 RESULTS OF THE PSHA FOR FORGE DRILLING CENTER

Figures 4-3, 4-4, 4-5 and 4-6 show the hazard results for the FORGE drilling center respectively for PGA, and 5 Hz, 1 Hz and 0.2 Hz spectral acceleration (or spectral periods of 20, 1, and 5 s). These ground-motion measures span the frequency range of primary interest. The figures show in black the total mean hazard curve defining the mean frequency of exceeding specified ground-motion levels over all the sources of uncertainty defined in Section 3. The range in the results is shown by curves defining the 5th (black, dash-dotted curve) and 95th (black, dashed curve) percentiles of the distributions for frequency of exceedance computed from the logic tree. These percentile hazard curves define uncertainty in the hazard resulting from uncertainties in specifying the inputs to the analysis. The contribution to the total mean hazard from various elements of the source characterization model are also shown on the figures. The blue curve represents the contribution from the areal source zones, which is dominated by the Basin and Range zone. The host zone is the largest contributor to the hazard at exceedance frequencies greater than 10-4. Below that level (return period of 10,000 years and greater) the local faults (light blue curve) become the largest contributors. This curve represents the combined

contribution of the Opal Mound, Negromag Wash and Mineral Mountain West faults. At 5 s (0.2 Hz), the Wasatch fault (orange curve) is the second largest contributor to the total hazard for short return periods (annual exceedance frequencies of 10^{-2} to 10^{-4}). The orange curves represent the overall Wasatch model obtained by combining the three modeling alternatives described in Section 3.1.3.1. In all figures, the green curve represents the aggregated contribution of all the regional faults (excluding Wasatch). Figure 4-5 shows the contribution of all the faults and fault segments to the total hazard at 1 Hz: aside from various segments of the Wasatch fault zone, and the three local sources, the regional fault that show the highest contribution is the Paragonah fault (PAR), which is located to the southeast of the FORGE drilling center.

A sensitivity test was conducted for the Mineral Mountain West fault to evaluate the sensitivity of the hazard to the mean slip rate. The test is conducted by assigning the highest weight to the lowest slip rate (0.002 mm/yr). Figure 4-7 shows that the hazard for this fault will be reduced by approximately 40%, which in turn will cause a reduction of the total hazard of approximately 10% for AFE of 10^{-4}.

Figure 4-8 shows the mean horizontal uniform hazard response spectra (UHRS) obtained by interpolation of the total mean hazard curves for the 10 spectral frequencies analyzed, at specified annual frequencies of 1/475 years, 1 /975 years, 1/2,475 years,1/5,000 years, and 1/10,000 years. The values are shown in Table 4-1.

Deaggregation of the seismic hazard is used to identify the mean M and mean distance of earthquakes contributing to the seismic hazard at a given spectral frequency and return period. The mean M and mean distance resulting from the deaggregation of the seismic hazard for PGA, 5 Hz, 1Hz, and 0.2 Hz (PGA, 20, 1, and 5 s) and for return periods of 475, 975, 2,475, 5,000 and 10,000 years are shown in Table 4-2.

4.4 RESULTS OF THE PSHA FOR THE WINDMILLS, MILFORD, AND BLUNDELL PLANT

The seismic hazard analyses were repeated for the windmills, the town of Milford, UT, and the Blundell Geothermal Plant using the appropriate site characterization. Seismic hazard curves for the windmills are shown in Figures 4-10 through 4-13, the UHRS is shown in Figure 4-14 and in Table 4-3. The deaggregation results for the windmills are shown in Table 4-4. The seismic hazard curves for the town of Milford, UT, are shown in Figures 4-15 through 4-18, the UHRS is

shown in Figure 4-19 and in Table 4-5. The deaggregation results for Milford are shown in Table 4-6. The seismic hazard curves for the Blundell Geothermal plant are shown in Figures 4-20 through 4-23, the UHRS is shown in Figure 4-24 and in Table 4-7. The deaggregation results for the Blundell plant are shown in Table 4-8.

Figure 4-25 compares the 475 years return period UHRS for the four sites analyzed in this study. The results are comparable for FORGE, Blundell Plant and Milford due to their proximity to each other, with differences mostly due to the different V_{S30}. The hazard obtained for the windmills, which are located to the north of the FORGE drilling center, is lower because the location is further away from the local sources, the Paragonah fault and the observed seismicity belt.

5.0 CONCLUSIONS

This report updates the design ground motions for the FORGE drilling center, the town of Milford, UT, a central location in the adjacent windmills, and the Blundell geothermal plant. The seismic hazard was calculated for the local site condition in terms of Peak Ground Acceleration and nine spectral frequencies ranging from 0.2 Hz (5 s) to 50 Hz (0.02 s), and then interpolated to obtain spectral accelerations at annual frequencies of 1/475, 1/975, 1/2,475, 1/5,000 and 1/10,000 years. The results for the FORGE drilling center, Milford, and the Blundell Geothermal Plant are very similar due to the proximity of the three sites. The results for the windmills are slightly lower due to its increased distance from the main seismicity, which is concentrated along the Intermountain Seismic Belt, the local faults and the Paragonah fault.

Magnitude and distance deaggregation confirm that for short return periods the high-frequency hazard is controlled by relatively small nearby earthquakes associated with the background seismicity zone (Basin and Range zone), while the low-frequency hazard is affected by larger M, more distant earthquakes, such as those occurring on the nearest segment of the Wasatch fault. For long return periods, the hazard is dominated by earthquakes occurring on the local faults.

6.0 REFERENCES

Abrahamson, N.A., Silva, W.J., and Kamai, R., 2014, Summary of the AKS14 Ground-Motion Relation for Active Crustal Regions, Earthquake Spectra, Vol. 30, DOI: 10.1193/070913EQS198M

Al Atik, L., and Youngs, R.R., 2014, Epistemic Uncertainty for NGA-West2 Models, Earthquake Spectra, 30(3), 1301-1318, DOI: 10.1193/062813EQS173M.

Amec Foster Wheeler, 2018, Probabilistic Seismic Hazard Assessment for the FORGE Site, Rev 0, prepared for the University of Utah, February 2018.

Arabasz, W.J., Pechman, J.C. and Burlacu, R., 2016, A uniform moment magnitude earthquake catalog and background seismicity rates for the Wasatch Front and surrounding Utah region: Appendix E in Working Group on Utah Earthquake Probabilities (WGUEP), 2016, Earthquake probabilities for the Wasatch front region in Utah, Idaho, and Wyoming: Utah Geological Survey Miscellaneous Publication 16-3, variously paginated.

Arabasz, W.J., Burlacu, R., and Pechman J.C., 2017, Earthquake database for Utah Geological Survey Map M-277: Utah earthquakes (1850-2016) and quaternary faults, May 15, 2017, 16 pp.

Bagge, M., Hampel, A., and R.D. Gold, 2019, Modeling the Holocene slip history of the Wasatch fault (Utah): Coseismic and postseismic Coulomb stress changes and implications for paleoseismicity and seismic hazard. GSA Bulletin, 131 (1-2): 43–57.

Bartley, J.M., 2019, Joint patterns in the Mineral Mountains intrusive complex and their roles in subsequent deformation and magmatism, in Allis, R., and Moore, J.N., editors, Geothermal characteristics of the Roosevelt Hot Springs system and adjacent FORGE EGS site, Milford, Utah: Utah Geological Survey Miscellaneous Publication 169-C, 13 p., 1 appendix.

Bennett, S.E.K., DuRoss, C. B., Gold, R. D., Briggs, R. W., Personius, S. F., Reitman, N. G., Devore, J. R., Hiscock, A. I., Mahan, S. A., Gray, H. J., Gunnarson, S., Stephenson, W. J., Pettinger, E., and J. K. Odum, 2018, Paleoseismic Results from the Alpine Site, Wasatch Fault Zone: Timing and Displacement Data for Six Holocene Earthquakes at the Salt Lake City–Provo Segment Boundary. Bulletin of the Seismological Society of America; 108 (6): 3202–3224.

Boore, D.M., Stewart, J.P., Seyhan, E., and Atkinson, G.M., 2014, NGA-West 2 Equations for Predicting PGA, PGV, and 5%-Damped PSA for Shallow Crustal Earthquakes, Earthquake Spectra, DOI: 10.1193/070113EQS184M

Bozorgnia, Y., Abrahamson, N.A., Al Atik, L., Ancheta, T.D, Atkinson, G.M., Baker, J.W., Baltay, A., Boore, D.M., Campbell, K.W., Chiou, B.S.-J., Darragh, R., Day, S., Donahue, J., Graves, R.W., Gregor, N., Hanks. T., Idriss, I.M., Kamai, R., Kishida, T., Kottke, A., Mahin, S.A., Rezaeian, S., Rowshandel, B., Seyhan, S., Shahi, S., Shantz, T., Silva, W., Spudich, P., Stewart, J.P., Watson-Lamprey, J., Wooddell, K, and Youngs, R.R., 2014, NGA-West2 research project, Earthquake Spectra, v, 30(3), p. 973-987.

Bruno, P.P.G., DuRoss, C.B., and S. Kokkalas, 2017, High-resolution seismic profiling reveals faulting associated with the 1934 Ms 6.6 Hansel Valley earthquake (Utah, USA). GSA Bulletin; 129 (9-10): 1227–1240.

Budnitz, R.J., Apostolakis, G., Boore, D.M., Cluff, L.S., Coppersmith, K.J., Cornell, C.A., and Morris, P.A., 1997. Recommendations for Probabilistic Seismic Hazard Analysis: Guidance on Uncertainty and Use of Experts, Report NUREG/CR-6372, Lawrence Livermore National Laboratory, sponsored by the U.S. Nuclear Regulatory Commission, U.S. Department of Energy, and Electric Power Research Institute.

Campbell, K.W., and Bozorgnia, Y., 2014, NGA-West2 Ground Motion Model for the Average Horizontal Components of PGA, PGV, and 5%-Damped Linear Acceleration Response Spectra, Earthquake Spectra, Vol. 30, DOI: 10.1193/062913EQS175M

Chiou, B.S-J., and Youngs, R.R., 2014, Update of the Chiou and Youngs NGA Model for the Average Horizontal Component of Peak Ground Motion and Response Spectra, Earthquake Spectra, Vol. 30, DOI: 10.1193/072813EQS219M

Cornell, C.A. 1968. Engineering seismic risk analysis. Bulletin of the Seismological Society of America 58 (5), 1583-1606.

Cornell, C.A. 1971. Probabilistic Analysis of Damage to Structures under Seismic Loads: in Howells, D.A., I.P. Haigh, and C. Taylor (editors), Dynamic Waves in Civil Engineering. Proceedings of a Conference Organized by the Society for Earthquake and Civil Engineering Dynamics, John Wiley, New York, pp. 473-493.

Duross, C., Hylland, M.D., Hiscock, A., Personius, S., Briggs, R.W., Gold, R.D., Beukelman, G., McDonald, G.N., Erickson, B., McKean, A., Angster, S., King, R., Crone, A.J., and S. A. Mahan, 2017, Holocene surface-faulting earthquakes at the Spring Lake and North Creek Sites on the Wasatch Fault Zone: Evidence for complex rupture of the Nephi Segment, Utah geological Survey Report, 28, 119 pp.

Duross, C., Personius, S., Olig, S.S., Crone, A.J., Hylland, M.D., Lund, W.R., and D. P. Schwartz, 2017, The history of late Holocene surface-faulting earthquakes on the central segments of the Wasatch fault zone, Utah: in Geology and resources of the Wasatch: Back to front, Utah Geological Association Publication 46, 1-51.

Electric Power Research Institute (EPRI). 2006. Program on Technology Innovation: Truncation of the Lognormal Distribution and Value of the Standard Deviation for Ground Motion Models in the Central and Eastern United States. EPRI Report 1013105, Technical Update, February, Palo Alto, Calif.

Electric Power Research Institute and Seismic Owners Group (EPRI-SOG). 1988. Seismic Hazard Methodology for Central and Eastern United States. EPRI-NP 4726, 10 vols.

Electric Power Research Institute (EPRI), U.S. Department of Energy, and U.S. Nuclear Regulatory Commission (EPRI/DOE/NRC). 2012. Technical Report: Central and Eastern United States Seismic Source Characterization for Nuclear Facilities. NUREG 2115.

Fay, M.P., 2010. Two-sided exact tests and matching confidence intervals for discrete data: The R Journal, v. 2, no. 1, pp. 53-58.

Gardner, J.K., and L. Knopoff. 1974. Is the sequence of earthquakes in Southern California, with aftershocks removed, Poissonian? Bulletin of the Seismological Society of America 80, 757-783.

Grünthal, G. 1985. The updated earthquake catalog for the German Democratic Republic and Adjacent Areas—Statistical Data Characteristics and Conclusions for Hazards Assessment: Proceedings 3rd International Symposium on the Analysis of Seismicity and Seismic Risk, Czechoslovak Academy of Sciences, Prague, p. 19-25.

Hanks, T.C. and Bakun, W.H., 2008, M − log A observations of recent large earthquakes, Bulletin of the Seismological Society of America, v. 98, p. 490-494.

Hecker, S., DuRoss, C.B., Schwartz, D.P., Cinti, F.R., Civico, R., Lund, W.R., Hiscock, A.I., West, M.W., Wilcox, T., and A. R. Stoller, 2019, Stratigraphic and Structural Relations in Trench Exposures and Geomorphology at the Big Burn, Lily Lake, and Lester Ranch Sites, Bear River Fault Zone, Utah and Wyoming, USGS Scientific Investigations Map 3430, 3 Maps, 1 Pamphlet.

Howe, J.C., 2017. Characterization of Segmentation and Long-Term Vertical Slip Rates of the Wasatch Fault Zone, Utah. Master's Thesis, University of Utah

Howe, J., Jewell, P., and R. Bruhn, 2019, Late Pleistocene Record of Off-Fault Deformation and Vertical Slip Rates from the Wasatch Fault Zone, Utah: Implications for Fault Segmentation from Lake Bonneville Shorelines. Bulletin of the Seismological Society of America; 109 (6): 2198–2215.

Keefer, DI, and SE Bodily. 1983. Three-point approximations for continuous random variables. Management Science 26(5):595−609.

Kleber, E. 2017. Information for PSHA analysis for Utah FORGE project area. Letter Utah Geological Survey. 9 pp.

Knudsen, T., Kleber, E., Hiscock, A., and S.M. Kirby, 2019, Quaternary geology of the Utah FORGE site and vicinity, Millard and Beaver Counties, Utah, in Allis, R., and Moore, J.N., editors, Geothermal characteristics of the Roosevelt Hot Springs system and adjacent FORGE EGS site, Milford, Utah: Utah Geological Survey Miscellaneous Publication 169-B, 21 p.

Kulkarni, R.B., Youngs, R.R., and Coppersmith, K.J., 1984, Assessment of confidence intervals for results of seismic hazard analysis: Proceedings of the Eighth World Conference on Earthquake Engineering, San Francisco, Calif., v. 1, pp. 263-270.

McDonald, G.N., Hiscock, A.I., Kleber, E.J., and S. D. Bowman, 2018, Detailed Mapping of The Wasatch Fault Zone, Utah and Idaho—Using New High-Resolution Lidar Data to Reduce Earthquake Risk, Final Technical Report, Award number G17AP00001, 21 pp.

Peck, A., 2018, Miocene-Quaternary Deformation along the Central Maynard Lake Fault, Pahranagat Shear Zone, Nevada: Master's Thesis, UNLV, 84 pp.

Petersen, M.D., Moschetti, M.P., Powers, P.M., Mueller, C.S., Haller, K.M., Frankel, A.D., Zeng, Y., Rezaeian, S., Harmsen, S.C., Boyd, O.S., Field, Ned, Chen, R., Rukstales, K.S., Luco, N., Wheeler, R.L., Williams, R.A., and Olsen, A.H., 2014, Documentation for the 2014 update of the United States National Seismic Hazard Maps: U.S. Geological Survey Open-File Report 2014–1091, 243 pp., http://dx.doi.org/10.333/ofr20141091

Petersen, M. D., Shumway, A. M., Powers, P. M., Mueller, C. S., Moschetti, M. P., Frankel, A. D., Rezaeian,S., McNamara D.E., Luco, N., Boyd, O.S., Rukstales K.S., Jaiswal, K.S., Thompson E.M., Hoover, S.M., Clayton B.S., Field, E.H., and Y. Zeng, 2019, The 2018 update of the US National Seismic Hazard Model: Overview of model and implications, Earthquake Spectra, 36(1), 5–41. https://doi.org/10.1177/8755293019878199

Silverman, B.W., 1986, Density Estimation for Statistics and Data Analysis, Chapman and Hall, London.

Stirling, M., Rhoades, D., and K. Berryman, 2002, Comparison of earthquake scaling derived from data of the instrumental and preinstrumental era, Bulletin of the Seismological Society of America, v. 92, p. 812-830.

Stock, C. and Smith, E.G.C., 2002, Adaptive kernel estimation and continuous probability representation of historical earthquake catalogs: Bulletin of the Seismological Society of America, vol. 92, p. 913-922.

Uhrhammer, R.A.1986. Characteristics of northern and central California seismicity (abs.). Earthquake Notes 57:21.

Valentini, A., DuRoss, C.B., Pace, B., Gold, R.D., Visini, F., Briggs, R.W., and Field, E.H., in press, Relaxing segmentation on the Wasatch fault zone: Impact on seismic hazard: Bulletin of the Seismological Society of America, manuscript BSSA-D-19-00088.

Veneziano, D., and Van Dyck, J., 1985, Analysis of earthquake catalogs for incompleteness and recurrence rates, Seismic Hazard Methodology for Nuclear Facilities in the Eastern United States, EPRI Research Projects N. P101-29, Electric Power Research Institute Seismic Owners Group Draft 85-1, v.2, Appendix A-6. Electric Power Research Institute, Palo Alto, California.

Weichert, D.H., 1980, Estimation of the Earthquake Recurrence Parameters for Unequal Observation Periods for Different Magnitudes: Bulletin of the Seismological Society of America, vol. 70, p. 1337–1346.

Wesnousky, S.G., 2008, Displacement and geometrical characteristics of earthquake surface ruptures–Issues and implications for seismic-hazard analysis and the process of earthquake rupture, Bulletin of the Seismological Society of America, v, 98, p. 1609-1632.

Working Group on Utah Earthquake Probabilities (WGUEP), 2016, Earthquake probabilities for the Wasatch Front region in Utah, Idaho, and Wyoming: Utah Geological Survey Miscellaneous Publication 16-3, 164 pp., 5 appendices.

Youngs, R.R. and Coppersmith, K.J., 1985, Implications of fault slip rates and earthquake recurrence models to probabilistic seismic hazard estimates: Bulletin of the Seismological Society of America, v. 75, no. 4, p. 939-964.

Zhang, H., Pankow, K., and Stephenson, W., 2019, A Bayesian Monte Carlo inversion of spatial auto-correlation (SPAC) for near-surface Vs structure applied to both broad-band and geophone data: Geophys. J. Int. (2019) 217, 2056-2070.

TABLE 1-1

COORDINATES OF THE SITES USED IN THE PSHA

University of Utah

Salt Lake City, Utah

Site	Latitude	Longitude
FORGE drill center	38°30'09.5"N	112°53'17.86"W
Milford, UT	38°23'49.43"N	113° 0'51.64"W
Blundell Geothermal Plant	38°29'20.06"N	112°51'10.70"W
Windmills	38°34'50.25"N	112°55'24.88"W

TABLE 2-1

EFFECT OF USING ALTERNATIVE CATALOG DECLUSTERING METHODS

University of Utah

Salt Lake City, Utah

Magnitude Interval	Original Catalog	Grünthal (1985)	Gardned and Knopoff (1974)	Urhammer (1983)	Veneziano and Van Dyke (1985)
2.0-2.3	28,358	13,410	16,372	21,757	10,709
2.3-2.6	1,108	544	636	779	462
2.6-2.9	1,006	472	538	670	425
2.9-3.2	882	458	530	626	369
3.2-3.5	653	324	368	443	291
3.5-3.8	363	222	239	278	206
3.8-4.1	207	131	135	147	114
4.1-4.4	70	53	53	57	37
4.4-4.7	41	25	25	26	17
4.7-5.0	38	21	23	25	23
5.0-5.3	17	9	10	11	7
5.3-5.6	13	10	10	10	10
5.6-5.9	2	1	1	1	1
5.9-6.2	2	2	2	2	0
6.2-6.5	1	1	1	1	1
6.5-6.8	2	2	2	2	2
6.8-7.1	0	0	0	0	0
Total	**32,763**	**15,685**	**18,945**	**24,835**	**12,674**

TABLE 2-2

COMPLETENESS INTERVALS
University of Utah
Salt Lake City, Utah

M interval	Beginning of Complete Period
WGUEP (2016)	
2.9≤M<3.6	1986
3.6≤M<4.3	1979
4.3≤M<5.0	1963
5.0≤M<5.7	1908
5.7≤M<6.4	1880
6.4≤M<7.0	1850
UTR (Arabasz et al., 2016)	
2.9≤M<3.6	1986
3.6≤M<4.3	1986
4.3≤M<5.0	1963
5.0≤M<5.7	1908
5.7≤M<6.4	1880
6.4≤M<7.0	1860

TABLE 2-3

RESULTS OF THE ONE-SIDED POISSON TEST FOR t=1.3
University of Utah
Salt Lake City, Utah

Magnitude	n_{obs}	$N>n\|\lambda_i$	$P[N>n_{obs}\|\ \lambda_i]$
M>3	13	11.87	77%
M≥3.55	3	4.16	91%

TABLE 3-1

SOURCE PARAMETERS FOR AREAL SOURCE ZONES

University of Utah
Salt Lake City, Utah

Zone	Style of Faulting[1]	Average Fault Trend	Average Dip[1]	Dip Direction[1]	Top Depth of Rupture (km)	Maximum Depth of Seismogenic Rupture (km) [2]	Maximum Observed Earthquake	Maximum Magnitude Distribution[2]
Basin and Range	N (0.7) SS (0.3)	N30E	For Normal: 35 (0.2) 50 (0.6) 65 (0.2) For Strike-Slip: 90 (1.0)	Equally likely in both direction. Vertical	0	8 (0.2) 12 (0.6) 16 (0.2)	6.63 (1901/11/14)	6.75 (0.3) 7.00 (0.4) 7.25 (0.3)
Colorado Plateau	N (0.5) SS (0.5)	Random	For Normal: 35 (0.2) 50 (0.6) 65 (0.2) For Strike-Slip: 90 (1.0)	Equally likely in both direction. Vertical	0	8 (0.2) 12 (0.6) 16 (0.2)	5.02 (1988/8/14)	6.75 (0.3) 7.00 (0.4) 7.25 (0.3)
Rocky Mountains	N (0.5) SS (0.5)	Random	For Normal: 35 (0.2) 50 (0.6) 65 (0.2) For Strike-Slip: 90 (1.0)	Equally likely in both direction. Vertical	0	8 (0.2) 12 (0.6) 16 (0.2)	5.3 (1950/1/18)	6.75 (0.3) 7.00 (0.4) 7.25 (0.3)

Notes

1. Aleatory variability distribution.
2. Epistemic uncertainty distribution.

TABLE 3-2

SOURCE PARAMETERS FOR LOCAL AND REGIONAL FAULTS

University of Utah

Salt Lake City, Utah

Fault Name	Code	P_a[1]	Style of Faulting	Average Dip[2] (deg)	Dip Direction	Rupture Length (km)	Slip Rate[2] (mm/yr)
Opal Mound fault	OPM	1	Normal	35 (0.2) 50 (0.6) 65 (0.2)	E	5	0.002 (0.125) 0.060 (0.75) 0.200 (0.125)
Negro Mag Wash fault	NMW	0.4	Normal	35 (0.2) 50 (0.6) 65 (0.2)	N	10	0.002 (0.125) 0.060 (0.75) 0.200 (0.125)
Mineral Mountain West fault zone	MMW	1	Normal	35 (0.2) 50 (0.6) 65 (0.2)	E and W	15	0.002 (0.125) 0.060 (0.75) 0.200 (0.125)
Antelope Range-Kingsley Mountains fault zone	ARK	1	Normal	35 (0.2) 50 (0.6) 65 (0.2)	E	69	0.013 (0.8) 0.300 (0.1) 0.020 (0.1)
Aubrey fault zone	AUB	1	Normal	35 (0.2) 50 (0.6) 65 (0.2)	W	63	0.023 (0.8) 0.030 (0.1) 0.040 (0.1)
Bear River fault zone	BRI	1	Normal	35 (0.2) 50 (0.6) 65 (0.2)	W	37	1.958 (0.8) 0.580 (0.1) 0.680 (0.1)
Black Hills fault	BLH	1	Normal	35 (0.2) 50 (0.6) 65 (0.2)	SE	9	0.131 (0.8) 0.170 (0.1) 0.110 (0.1)
Butte Mountains fault zone	BUM	1	Normal	35 (0.2) 50 (0.6) 65 (0.2)	W	61	0.013 (0.8) 0.220 (0.1) 0.010 (0.1)
California Wash fault	CAW	1	Normal	35 (0.2) 50 (0.6) 65 (0.2)	W	34	0.366 (0.8) 0.200 (0.1) 0.480 (0.1)

TABLE 3-2

SOURCE PARAMETERS FOR LOCAL AND REGIONAL FAULTS

University of Utah

Salt Lake City, Utah

Fault Name	Code	P_a[1]	Style of Faulting	Average Dip[2] (deg)	Dip Direction	Rupture Length (km)	Slip Rate[2] (mm/yr)
Coyote Spring fault	COS	1	Normal	35 (0.2) 50 (0.6) 65 (0.2)	W	15	0.013 (0.8) 0.230 (0.1) 0.010 (0.1)
Diamond Mountains fault	DIM	1	Normal	35 (0.2) 50 (0.6) 65 (0.2)	E	83	0.131 (0.8) 0.110 (0.1) 0.170 (0.1)
Dry Lake fault	DRL	1	Normal	35 (0.2) 50 (0.6) 65 (0.2)	W	47	0.010 (0.8) 0.080 (0.1) 0.010 (0.1)
Dutchman Draw fault	DUD	1	Normal	35 (0.2) 50 (0.6) 65 (0.2)	NW	16	0.098 (0.8) 0.100 (0.1) 0.130 (0.1)
East Cache fault zone	EAC	1	Normal	35 (0.2) 50 (0.6) 65 (0.2)	W	81	0.261 (0.8) 0.350 (0.1) 0.280 (0.1)
East Great Salt Lake fault zone, Antelope section	SLA	1	Normal	35 (0.2) 50 (0.6) 65 (0.2)	W	38	0.550 (0.5) 0.880 (0.5)
East Great Salt Lake fault zone, Fremont Island section	SLF	1	Normal	35 (0.2) 50 (0.6) 65 (0.2)	W	32	0.780 (0.8) 0.460 (0.1) 1.080 (0.1)
East Great Salt Lake fault zone, Promontory section	SLP	1	Normal	35 (0.2) 50 (0.6) 65 (0.2)	W	53	0.260 (0.5) 1.190 (0.5)
Eglington fault	EGL	1	Normal	35 (0.2) 50 (0.6) 65 (0.2)	SE	10	0.160 (0.5) 0.030 (0.5)

TABLE 3-2

SOURCE PARAMETERS FOR LOCAL AND REGIONAL FAULTS

University of Utah

Salt Lake City, Utah

Fault Name	Code	P_a[1]	Style of Faulting	Average Dip[2] (deg)	Dip Direction	Rupture Length (km)	Slip Rate[2] (mm/yr)
Frenchman Mountain fault	FRM	1	Normal	35 (0.2) 50 (0.6) 65 (0.2)	W	20	0.020 (0.8) 0.120 (0.1) 0.030 (0.1)
Golden Gate fault	GOG	1	Normal	35 (0.2) 50 (0.6) 65 (0.2)	E	36	0.013 (0.8) 0.130 (0.1) 0.010 (0.1)
Hiko fault zone	HIK	1	Normal	35 (0.2) 50 (0.6) 65 (0.2)	W	15	0.013 (0.8) 0.100 (0.1) 0.010 (0.1)
Hurricane fault zone (central)	HUC	1	Normal	35 (0.2) 50 (0.6) 65 (0.2)	NW	106	0.261 (0.8) 0.300 (0.1) 0.360 (0.1)
Hurricane fault zone (northern)	HUN	1	Normal	35 (0.2) 50 (0.6) 65 (0.2)	NW	47	0.261 (0.8) 0.620 (0.1) 0.330 (0.1)
Hurricane fault zone (southern)	HUS	1	Normal	35 (0.2) 50 (0.6) 65 (0.2)	NW	98	0.106 (0.8) 0.100 (0.1) 0.160 (0.1)
Independence Valley fault zone	IND	1	Normal	35 (0.2) 50 (0.6) 65 (0.2)	W	66	0.131 (0.8) 0.120 (0.1) 0.160 (0.1)
Jakes Valley fault zone	JAV	1	Normal	35 (0.2) 50 (0.6) 65 (0.2)	E	36	0.013 (0.8) 0.090 (0.1) 0.010 (0.1)
Joes Valley fault zone east fault	JOV	1	Normal	35 (0.2) 50 (0.6) 65 (0.2)	W	47	0.261 (0.8) 0.230 (0.1) 0.290 (0.1)

TABLE 3-2

SOURCE PARAMETERS FOR LOCAL AND REGIONAL FAULTS

University of Utah

Salt Lake City, Utah

Fault Name	Code	P_a[1]	Style of Faulting	Average Dip[2] (deg)	Dip Direction	Rupture Length (km)	Slip Rate[2] (mm/yr)
Kane Spring Wash fault	KSW	1	Strike Slip	90 (1.0)	n/a	43	0.010 (0.8) 0.050 (0.1) 0.010 (0.1)
Morgan fault	MOR	1	Normal	35 (0.2) 50 (0.6) 65 (0.2)	W	17	0.026 (0.8) 0.030 (0.1) 0.040 (0.1)
Mount Irish Range fault	MIR	1	Normal	35 (0.2) 50 (0.6) 65 (0.2)	W	12	0.013 (0.8) 0.040 (0.1) 0.010 (0.1)
Northern Butte Valley fault	NBV	1	Normal	35 (0.2) 50 (0.6) 65 (0.2)	W	13	0.131 (0.8) 0.100 (0.1) 0.130 (0.1)
Northern Huntington Valley fault zone	NHV	1	Normal	35 (0.2) 50 (0.6) 65 (0.2)	W	39	0.131 (0.8) 0.170 (0.1) 0.120 (0.1)
Oquirrh-Southern Oquirrrh Mountains fault zone	OSM	1	Normal	35 (0.2) 50 (0.6) 65 (0.2)	W	61	0.261 (0.8) 0.260 (0.1) 0.330 (0.1)
Paragonah fault	PAR	1	Normal	35 (0.2) 50 (0.6) 65 (0.2)	NW	27	0.600 (0.8) 0.550 (0.1) 0.550 (0.1)
Penoyer fault	PEN	1	Normal	35 (0.2) 50 (0.6) 65 (0.2)	W	54	0.021 (0.8) 0.030 (0.1) 0.030 (0.1)
Railroad Valley fault zone	RRV	1	Normal	35 (0.2) 50 (0.6) 65 (0.2)	W	152	0.091 (0.8) 0.120 (0.1) 0.120 (0.1)

TABLE 3-2

SOURCE PARAMETERS FOR LOCAL AND REGIONAL FAULTS

University of Utah

Salt Lake City, Utah

Fault Name	Code	P_a[1]	Style of Faulting	Average Dip[2] (deg)	Dip Direction	Rupture Length (km)	Slip Rate[2] (mm/yr)
Ruby Mountains fault zone	RMT	1	Normal	35 (0.2) 50 (0.6) 65 (0.2)	W	73	0.366 (0.8) 0.180 (0.1) 0.330 (0.1)
Ruby Valley fault zone	RVL	1	Normal	35 (0.2) 50 (0.6) 65 (0.2)	E	78	0.131 (0.8) 0.190 (0.1) 0.190 (0.1)
Schell Creek Range fault system	SCR	1	Normal	35 (0.2) 50 (0.6) 65 (0.2)	E	101	0.131 (0.8) 0.280 (0.1) 0.190 (0.1)
Sevier/Toroweap fault zone (northern)	STN	1	Normal	35 (0.2) 50 (0.6) 65 (0.2)	W	87	0.052 (0.8) 0.440 (0.1) 0.500 (0.1)
Sevier/Toroweap fault zone (southern)	STS	1	Normal	35 (0.2) 50 (0.6) 65 (0.2)	W	168	0.144 (0.8) 0.120 (0.1) 0.190 (0.1)
Sheep Basin fault	SHB	1	Normal	35 (0.2) 50 (0.6) 65 (0.2)	W	22	0.057 (0.8) 0.070 (0.1) 0.080 (0.1)
Spruce Mountain Ridge fault zone	SMR	1	Normal	35 (0.2) 50 (0.6) 65 (0.2)	W	32	0.131 (0.8) 0.050 (0.1) 0.160 (0.1)
Stansbury fault zone	STA	1	Normal	35 (0.2) 50 (0.6) 65 (0.2)	W	54	0.522 (0.8) 0.510 (0.1) 0.590 (0.1)
Strawberry fault	STR	1	Normal	35 (0.2) 50 (0.6) 65 (0.2)	W	37	0.131 (0.8) 0.230 (0.1) 0.130 (0.1)

TABLE 3-2

SOURCE PARAMETERS FOR LOCAL AND REGIONAL FAULTS

University of Utah

Salt Lake City, Utah

Fault Name	Code	P_a[1]	Style of Faulting	Average Dip[2] (deg)	Dip Direction	Rupture Length (km)	Slip Rate[2] (mm/yr)
West Spring Mountains fault	WSM	1	Normal	35 (0.2) 50 (0.6) 65 (0.2)	W	49	0.059 (0.8) 0.090 (0.1) 0.090 (0.1)
West Valley fault	WEV	1	Normal	35 (0.2) 50 (0.6) 65 (0.2)	E	17	0.522 (0.8) 0.315 (0.1) 0.440 (0.1)
Western Diamond Mountains fault zone	WDM	1	Normal	35 (0.2) 50 (0.6) 65 (0.2)	W	64	0.131 (0.8) 0.080 (0.1) 0.160 (0.1)
White River Valley fault zone	WRV	1	Normal	35 (0.2) 50 (0.6) 65 (0.2)	W	102	0.059 (0.8) 0.020 (0.1) 0.080 (0.1)

Notes

1. Probability fault is seismogenic.
2. Epistemic uncertainty distribution.

TABLE 3-3

SOURCE PARAMETERS FOR THE WASATCH FAULT

University of Utah

Salt Lake City, Utah

Fault Name	Code	P_a[1]	Style of Faulting	Average Dip[2] (deg)	Dip Direction	Rupture Length[2] (km)	Slip Rate[2] (mm/yr)
Wasatch fault floating M~7.4	WAF	1	Normal	35 (0.2) 50 (0.6) 65 (0.2)	W	127	1.2 (1.0)
Wasatch fault partial segment rutpures	WFS	1	Normal	35 (0.2) 50 (0.6) 65 (0.2)	W	20 (0.3) 30 (0.3) 40 (0.3) 50 (0.1)	Slip rate of each segment
Wasatch fault Salt Lake City section	WAS	1	Normal	35 (0.2) 50 (0.6) 65 (0.2)	W	52	1.697 (0.8) 1.030 (0.1) 1.080 (0.1)
Wasatch fault, Brigham City section	WAB	1	Normal	35 (0.2) 50 (0.6) 65 (0.2)	W	41	2.089 (0.8) 0.700 (0.1) 1.190 (0.1)
Wasatch fault, Levan section	WAL	1	Normal	35 (0.2) 50 (0.6) 65 (0.2)	W	32	2.480 (0.8) 1.450 (0.1) 1.270 (0.1)
Wasatch fault, Nephi section	WAN	1	Normal	35 (0.2) 50 (0.6) 65 (0.2)	W	46	2.219 (0.4) 1.00 (0.4) 0.500 (0.2)
Wasatch fault, Provo section	WAP	1	Normal	35 (0.2) 50 (0.6) 65 (0.2)	W	77	2.611 (0.4) 1.500 (0.4) 0.700 (0.2)
Wasatch fault, Weber section	WAW	1	Normal	35 (0.2) 50 (0.6) 65 (0.2)	W	63	2.480 (0.8) 1.450 (0.1) 1.270 (0.1)

Notes

1. Probability fault is seismogenic.
2. Epistemic uncertainty distribution.

TABLE 3-4

LITERATURE REVIEW
University of Utah
Salt Lake City, Utah

Author	Year	Notes	Revise Model?
Duross et al.	2017	This report discusses paleoseismic trenches across the Nephi segment of the Wasatch fault. The authors conclude a mean recurrence of ~1.2–1.5 kyr and vertical slip rate of ~0.5–0.8 mm/yr. They also find that the northern and southern strands can and do rupture at the same time.	Yes. The interpreted slip rates are lower than the range of 2.219-0.610 mm/yr used in the model. The slip rates and weights were updated to 2.219 (0.4), 1.0 (0.4), and 0.5 (0.2)
Hecker et al.	2019	This pamphlet and three maps document paleoseismic trenches across the Bear River fault zone. They find evidence for three ruptures, one of which is younger and was not interpreted in earlier studies.	No. The study is not yet completed and analysis of ages and offset per event on the fault has not been completed.
McDonald et al.	2018	This technical report is a preliminary report of LiDAR mapping of the Wasatch fault.	No. This is a preliminary report and does not contain the finalized updated map of the Wasatch fault
Brumbaugh	2019	This article discuses a 2016 swarm of earthquakes that occurred in the Grand Wash basin, northwestern Arizona.	No. The focal mechanisms of the events were determined to be normal which is consistent with the characterization of the Basin and Range areal source zone
Duross et al.	2017	This book chapter discusses the Holocene earthquake history of the Wasatch fault. They conclude a mean vertical slip rate of 1.3-2.0 mm/yr for the central segments of the fault.	No. The slip rates for the fault are consistent with the distribution of rates from the model.
Bruno et al.,	2017	This article examines scarps related to the 1934 Ms 6.6 Hansel Valley earthquake. They interpret evidence for both	No. The Basin and Range areal source zone accounts for booth normal (0.7) and strike-slip (0.3) faulting. The 1934 event is included in the earthquake catalog.
Bagge et al.	2019	This article uses three-dimensional forward modeling of the Wasatch fault to determine how earthquakes change the Coulomb stress. They conclude the Brigham City, Salt Lake City, and Provo segments are most prone to failure in a Mw ≥ 6.8 earthquake.	No. The magnitude and paleoseismic data used in this study were used in the development of this model. The authors conclude that the results of this study indicate that "forward modeling of earthquake sequences may ultimately contribute to improved seismic hazard estimates."
DuRoss et al.	2019	This abstract discusses modeling of the complexity of the Wasatch fault and the ability of barriers along the fault to limit rupture length. They conclude ruptures can likely across proposed barriers on the Wasatch fault.	No. The ability of ruptures to continue through barriers is accounted for in the two branches for unsegmented rupture on the Wasatch fault.
Bennett et al.	2018	This article discusses a paeloseismic trench from the north end of the Provo segment of the Wasatch fault. The study concludes a recurrence interval of 0.2-1.8 kyr, with earthquakes as large as Mw 7.0 and a late Holocene vertical slip rate of 0.9 mm/yr (0.7–1.2 mm/yr).	Yes. The slip rate from this study is slightly lower than the slip rate used in the model (2.611-1.670) based on Petersen et al. (2014). The slip rates and weights were updated to 2.611 (0 .4), 1.5 (0.4), and 0.7 (0.2).
Howe et al.	2019	This article is the follow up to Howe (2017). It uses the same information and conclusions.	No.
Howe	2017	This Master's thesis looked at the elevation of paleolake shorelines and determined that there did not seem to be a barrier to rupture between the Brigham City and Weber segments of the Wasatch fault.	No. The ability of ruptures to continue through barriers is accounted for in the two branches for unsegmented rupture on the Wasatch fault.
Peck	2018	This Master's thesis studied the Maynard fault, a transfer fault in the Basin and Range region of Nevada. It concluded the fault offsets Quaternary and possibly Holocene sediments.	No. The thesis refines the mapping and structure of the Maynard and other faults but does not refine the slip rate, recurrence or other information necessary for addition to the model.
Zhang et al.	2019	This study uses a Bayesian model and data from seismic arrays in the near the FORGE sites to update the near-surface Vs profiles.	
Knudsen et al.	2019	This article discusses the three faults ones neat the Utah FORGE site—The Negro Mag fault, the Opal Mound fault and the Mineral Mountains West fault zone. The article concludes the Negro Mag fault may be pre-Quaternary. They conclude the most recent movement on the Opal Mound fault and the Mineral Mountains West fault is likely late Pleistocene age.	Yes. Based on the new information regarding the likely inactivity of the Negro Mag fault, the likelihood of activity of the fault is lowered to 0.4.

TABLE 3-4

LITERATURE REVIEW
University of Utah
Salt Lake City, Utah

Author	Year	Notes	Revise Model?
Petersen et al.	2019	This article summarizes the updates to the 2018 National Seismic Hazard Map. Updates include new ground motion models, an updated seismicity catalog, and for several deep sedimentary basins including the Salt Lake City region amplified shaking estimates of long period ground motions were incorporated. The individual fault sources were not updated.	No. The fault sources were not updated for the model. Section 1.1 discusses the need to update the model for source zones.
Valentini et al.	2019	This article uses UCERF3 methodology and applies it to the Wasatch fault to determine the variation in ground motion hazard from modeling a segmented vs unsegmented fault. They conclude the segmented model increases hazard by increasing the rate of M 6.2-6.8 events. The Unsegmented model allows larger (M 6.9-7.9), less frequent earthquakes. They conclude segmentation rather than slip rate or scaling relations had the largest control on seismic hazard.	No. Segmented and unsegmented variations of the Wasatch fault are included in the model.

TABLE 3-5

SITE-SPECIFIC NGA-WEST 2 PARAMETERS
University of Utah
Salt Lake City, Utah

Site	V_{S30} (m/s)	$Z_{1.0}$ (m)	$Z_{2.5}$ (km)
FORGE drill center	448	293	1.00
Blundell Plant	401	80	1.08
Milford	315	246	1.246
Wind Farm	422	325	1.95

TABLE 4-1

MEAN HORIZONTAL UNIFORM HAZARD RESPONSE SPECTRA FOR THE FORGE DRILLING CENTER

University of Utah

Salt Lake City, Utah

Period (s)	Frequency (Hz)	475 years Return Period	975 years Return Period	2,475 years Return Period	5,000 years Return Period	10,000 years Return Period
0.01	100	0.1144	0.1774	0.3028	0.4268	0.5659
0.02	50	0.1162	0.1807	0.3087	0.4360	0.5780
0.05	20	0.1591	0.2468	0.4157	0.5783	0.7758
0.075	13.33	0.2060	0.3170	0.5256	0.7337	0.9745
0.1	10	0.2400	0.3673	0.6079	0.8475	1.1249
0.2	5	0.2715	0.4226	0.7244	1.0312	1.3900
0.5	2	0.1543	0.2439	0.4424	0.6672	0.9537
1	1	0.0733	0.1165	0.2151	0.3378	0.5013
2	0.5	0.0309	0.0482	0.0859	0.1313	0.1980
5	0.2	0.0083	0.0129	0.0222	0.0328	0.0461

TABLE 4-2

MEAN M AND MEAN DISTANCE (R) DEAGGREGATION FOR FORGE DRILLING CENTER

University of Utah

Salt Lake City, Utah

Period (s)	Frequency (Hz)	475 years Return Period	975 years Return Period	2,475 years Return Period	5,000 years Return Period	10,000 years Return Period
0.01	100	M 4.9, R 10 km	M 6.1, R 5 km	M 6.1, R 5 km	M 6.7, R 5 km	M 6.7, R 5 km
0.2	5	M 6.1, R 5 km	M 6.1, R 5 km	M 6.1, R 5 km	M 6.1, R 5 km	M 6.7, R 5 km
1	1	M 6.7, R 75 km	M 6.1, R 5 km	M 6.2, R 5 km	M 6.7, R 5 km	M 6.7, R 5 km
5	0.2	M7.1, R 200 km	M 7.3, R 200 km	M 6.7, R 5 km	M 6.7, R 5 km	M 6.7, R 5 km

TABLE 4-3

MEAN HORIZONTAL UNIFORM HAZARD RESPONSE SPECTRA FOR THE WINDMILLS

University of Utah

Salt Lake City, Utah

Period (s)	Frequency (Hz)	475 years Return Period	975 years Return Period	2,475 years Return Period	5,000 years Return Period	10,000 years Return Period
0.01	100	0.0970	0.1427	0.2292	0.3142	0.4138
0.02	50	0.0984	0.1449	0.2329	0.3195	0.4210
0.05	20	0.1319	0.1986	0.3152	0.4292	0.5611
0.075	13.33	0.1707	0.2545	0.4046	0.5463	0.7175
0.1	10	0.2022	0.3006	0.4731	0.6387	0.8379
0.2	5	0.2340	0.3502	0.5645	0.7786	1.0298
0.5	2	0.1407	0.2127	0.3523	0.5023	0.6868
1	1	0.0689	0.1053	0.1753	0.2535	0.3563
2	0.5	0.0305	0.0444	0.0725	0.1044	0.1446
5	0.2	0.0083	0.0124	0.0196	0.0279	0.0376

TABLE 4-4

MEAN M AND MEAN DISTANCE (R) DEAGGREGATION FOR WINDMILLS

University of Utah

Salt Lake City, Utah

Period (s)	Frequency (Hz)	475 years Return Period	975 years Return Period	2,475 years Return Period	5,000 years Return Period	10,000 years Return Period
0.01	100	M 5.8, R 15 km	M 6.7, R 15 km	M 6.7, R 15 km	M 6.7, R 15 km	M 6.7, R 15 km
0.2	5	M 5.8, R 15 km	M 5.9, R 15 km	M 6.7, R 15 km	M 6.7, R 15 km	M 6.7, R 15 km
1	1	M 6.9, R 150 km	M 6.6, R 15 km	M 6.7, R 15 km	M 6.7, R 15 km	M 6.7, R 15 km
5	0.2	M 6.9, R 150 km	M 7.0, R 150 km	M 6.7, R 15 km	M 6.7, R 15 km	M 6.7, R 15 km

TABLE 4-5

MEAN HORIZONTAL UNIFORM HAZARD RESPONSE SPECTRA FOR MILFORD, UT

University of Utah

Salt Lake City, Utah

Period (s)	Frequency (Hz)	475 years Return Period	975 years Return Period	2,475 years Return Period	5,000 years Return Period	10,000 years Return Period
0.01	100	0.1279	0.1955	0.3172	0.4356	0.5683
0.02	50	0.1291	0.1979	0.3210	0.4410	0.5750
0.05	20	0.1688	0.2554	0.4101	0.5538	0.7263
0.075	13.33	0.2173	0.3249	0.5129	0.6890	0.8960
0.1	10	0.2569	0.3796	0.5955	0.8018	1.0372
0.2	5	0.3142	0.4720	0.7557	1.0240	1.3302
0.5	2	0.1977	0.3046	0.5201	0.7582	1.0547
1	1	0.0933	0.1448	0.2539	0.3835	0.5557
2	0.5	0.0372	0.0569	0.0986	0.1477	0.2176
5	0.2	0.0093	0.0141	0.0239	0.0347	0.0484

TABLE 4-6

MEAN M AND MEAN DISTANCE (R) DEAGGREGATION FOR MILFORD, UT

University of Utah

Salt Lake City, Utah

Period (s)	Frequency (Hz)	475 years Return Period	975 years Return Period	2,475 years Return Period	5,000 years Return Period	10,000 years Return Period
0.01	100	M 4.8, R 10 km	M 5.0, R 10 km	M 6.6, R 10 km	M 6.6, R 10 km	M 6.6, R 10 km
0.2	5	M 4.9, R 10 km	M 6.4, R 10 km	M 6.4, R 10 km	M 6.6, R 10 km	M 6.6, R 10 km
1	1	M 6.6, R 50 km	M 6.4, R 10 km	M 6.6, R 10 km	M 6.6, R 10 km	M 6.6, R 10 km
5	0.2	M 7.2, R 300 km	M 7.3, R 300 km	M 6.6, R 10 km	M 6.6, R 10 km	M 6.6, R 10 km

TABLE 4-7

MEAN HORIZONTAL UNIFORM HAZARD RESPONSE SPECTRA FOR THE BLUNDELL GEOTHERMAL PLANT

University of Utah

Salt Lake City, Utah

Period (s)	Frequency (Hz)	475 years Return Period	975 years Return Period	2,475 years Return Period	5,000 years Return Period	10,000 years Return Period
0.01	100	0.1262	0.1958	0.3322	0.4704	0.6233
0.02	50	0.1281	0.1991	0.3384	0.4801	0.6360
0.05	20	0.1730	0.2668	0.4461	0.6194	0.8278
0.075	13.33	0.2230	0.3408	0.5590	0.7786	1.0308
0.1	10	0.2615	0.3968	0.6503	0.9005	1.1913
0.2	5	0.3040	0.4698	0.7942	1.1218	1.5085
0.5	2	0.1710	0.2711	0.4945	0.7531	1.0708
1	1	0.0770	0.1235	0.2309	0.3673	0.5464
2	0.5	0.0293	0.0464	0.0840	0.1296	0.1968
5	0.2	0.0072	0.0114	0.0199	0.0302	0.0421

TABLE 4-8

MEAN M AND MEAN DISTANCE (R) DEAGGREGATION FOR BLUNDELL GEOTHERMAL PLANT

University of Utah

Salt Lake City, Utah

Period (s)	Frequency (Hz)	475 years Return Period	975 years Return Period	2,475 years Return Period	5,000 years Return Period	10,000 years Return Period
0.01	100	M 6.1, R 5 km	M 6.1, R 5 km	M 6.1, R 5 km	M 6.1, R 5 km	M 6.1, R 5 km
0.2	5	M 6.1, R 5 km	M 6.1, R 5 km	M 6.1, R 5 km	M 6.1, R 5 km	M 6.1, R 5 km
1	1	M 6.6, R 75 km	M 6.1, R 5 km	M 6.1, R 5 km	M 6.2, R 5 km	M 6.2, R 5 km
5	0.2	M 7.1, R 200 km	M 6.8, R 75 km	M 6.2, R 5 km	M 6.7, R 5 km	M 6.7, R 5 km

FIGURES

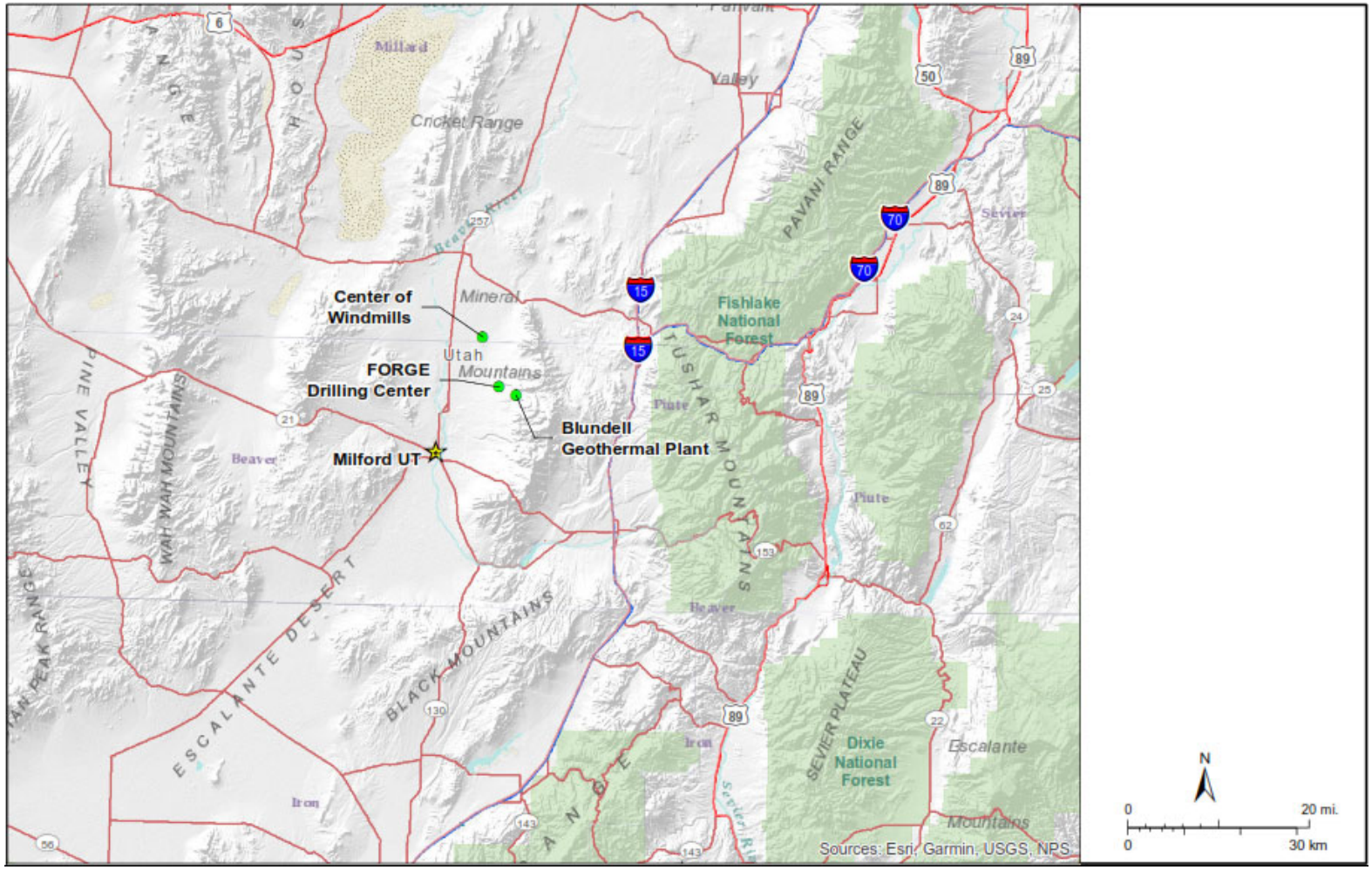

Figure 1-1: Site Location

Name	Region	Duplicate	Dependent	Anthro. M&E	Anthro. PFI
2014_emm.c2	CEUS	❌	✅	❌	✅
2014_emm.c3	CEUS	❌	❌	❌	✅
2014_emm.c4	CEUS	❌	❌	❌	❌
2014_wmm.c2	WUS	❌	✅	❌	✅
2014_wmm.c3	WUS	❌	❌	❌	✅
2014_wmm.c4	WUS	❌	❌	❌	❌

✅ = events included
❌ = events deleted
WUS = Western US
CEUS = Central & Eastern US

Figure 2-1: Characteristics of the Six NSHM Catalogs (Source: https://github.com/usgs/nshmp-haz-catalogs, accessed July 6, 2017)

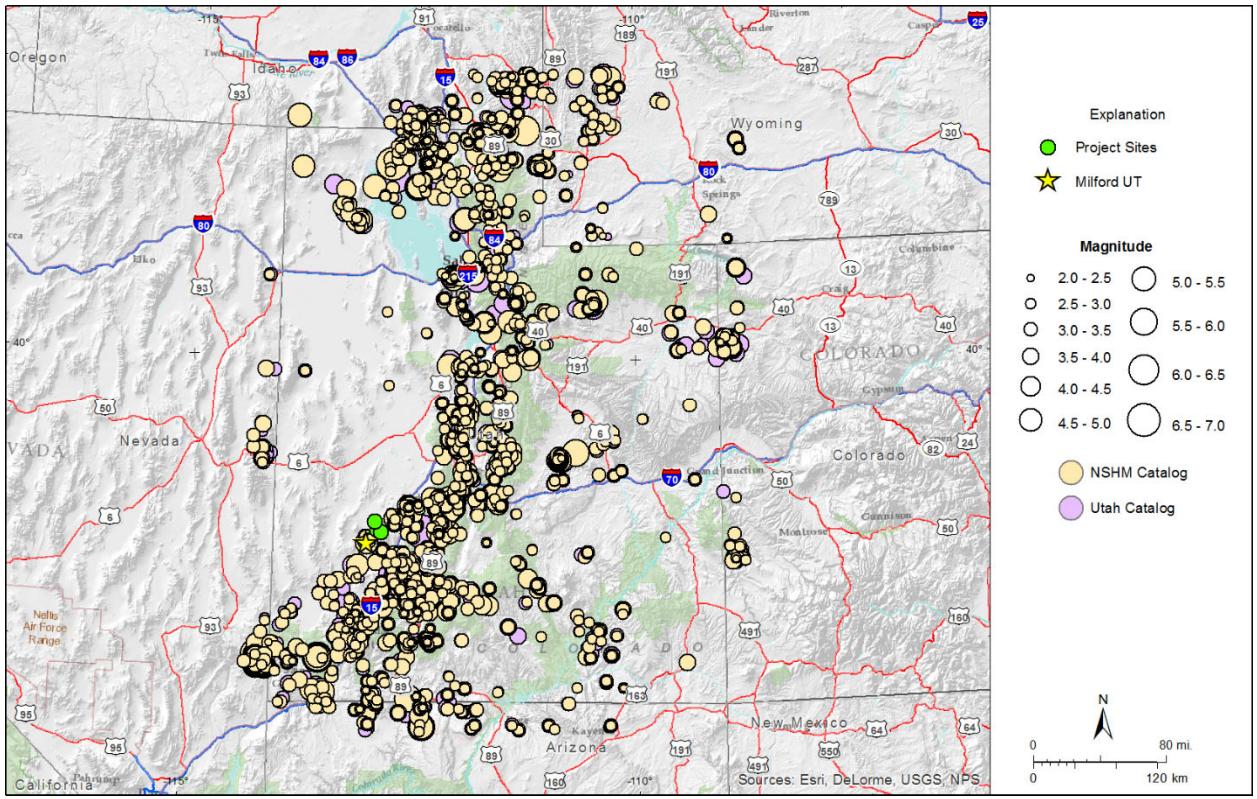

Figure 2-2: Earthquakes Common to the Utah (Black Circles) and NSHM (Green Circles) Catalogs

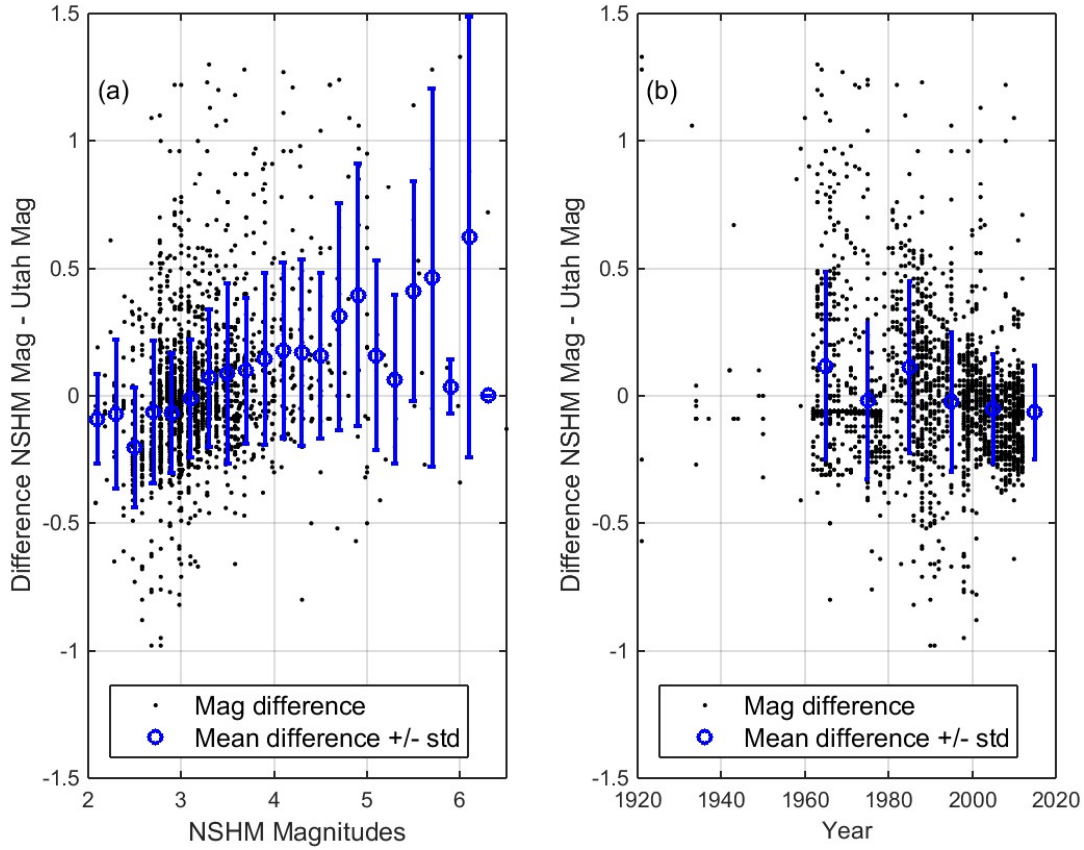

Figure 2-3: Difference in Magnitude Between Earthquakes in NSHM and Utah Catalog as a Function of Magnitude and Time

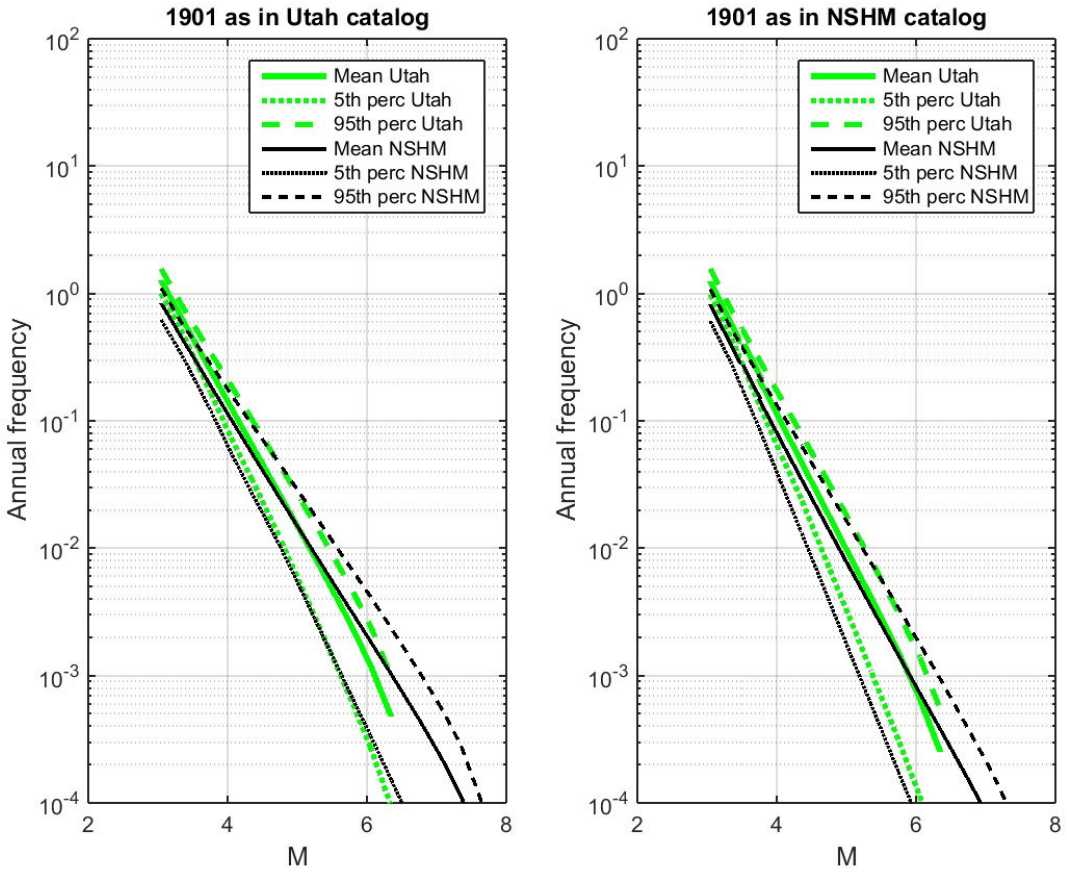

Figure 2-4: Comparison Between the Recurrence Within an Area of 50-km Radius Around FORGE Calculated from the NSHM Catalog (Black) and the Utah Catalog (Green)

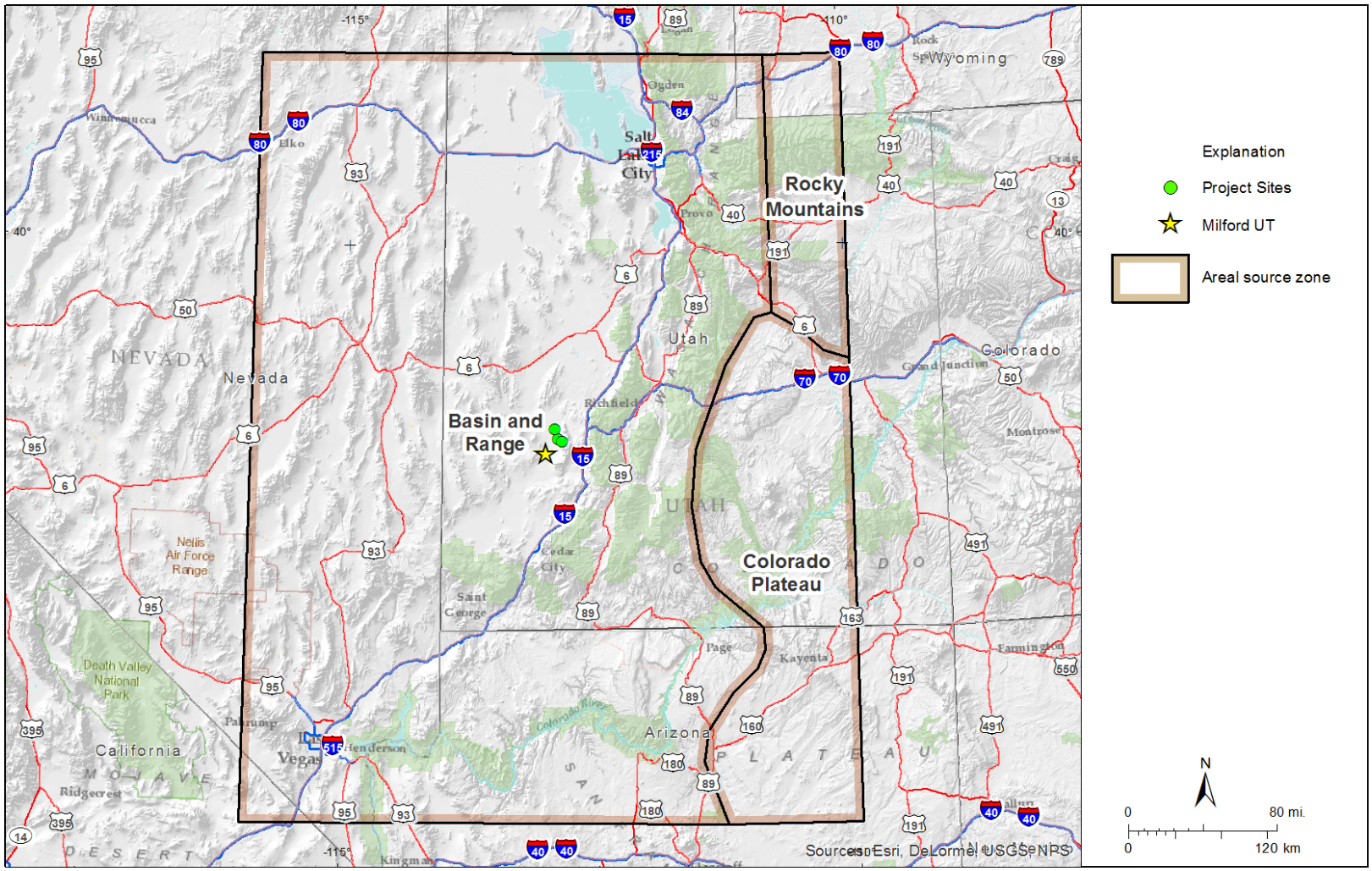

Figure 3-1: Areal Source Zones

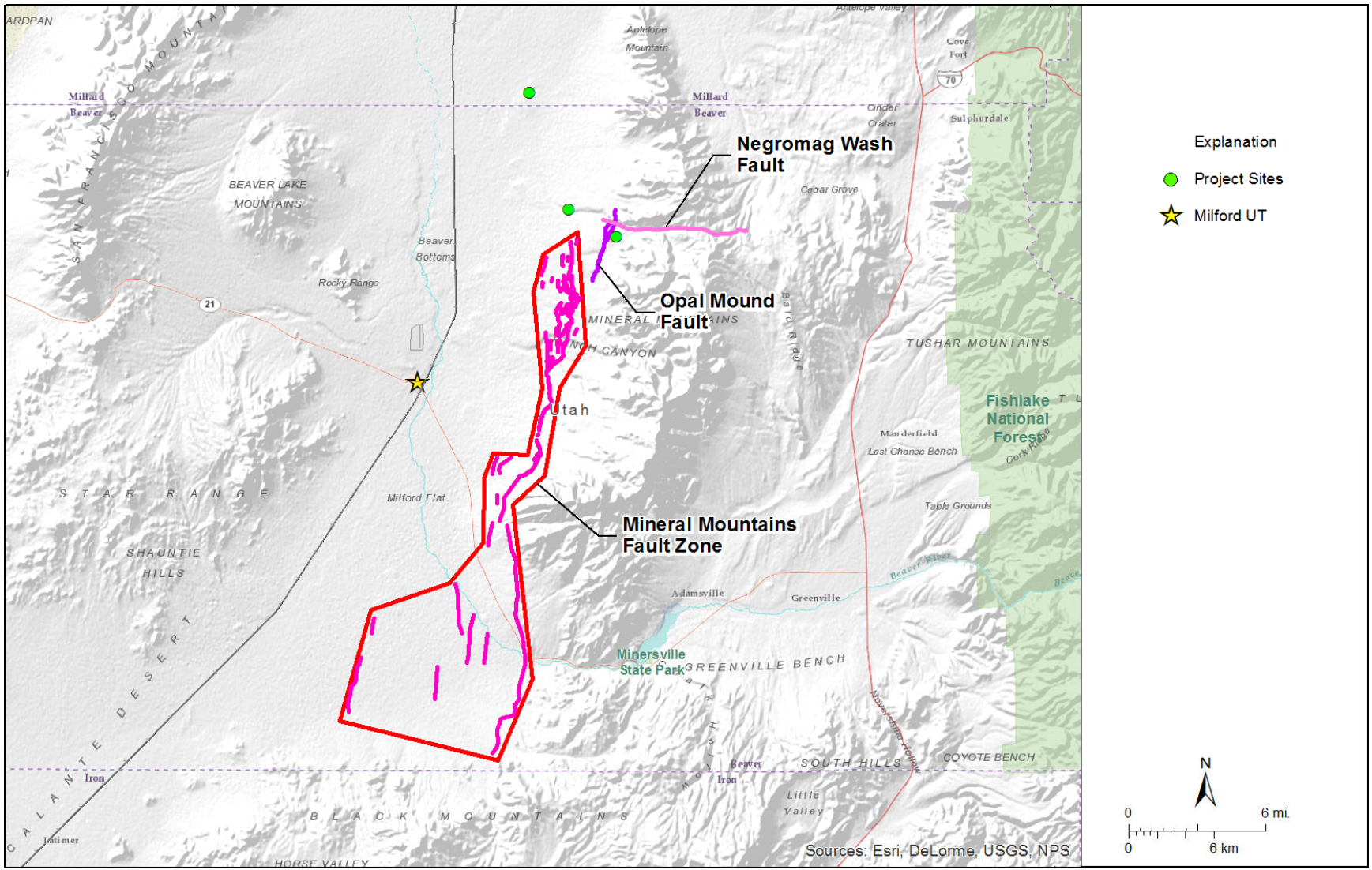

Figure 3-2: Local Faults

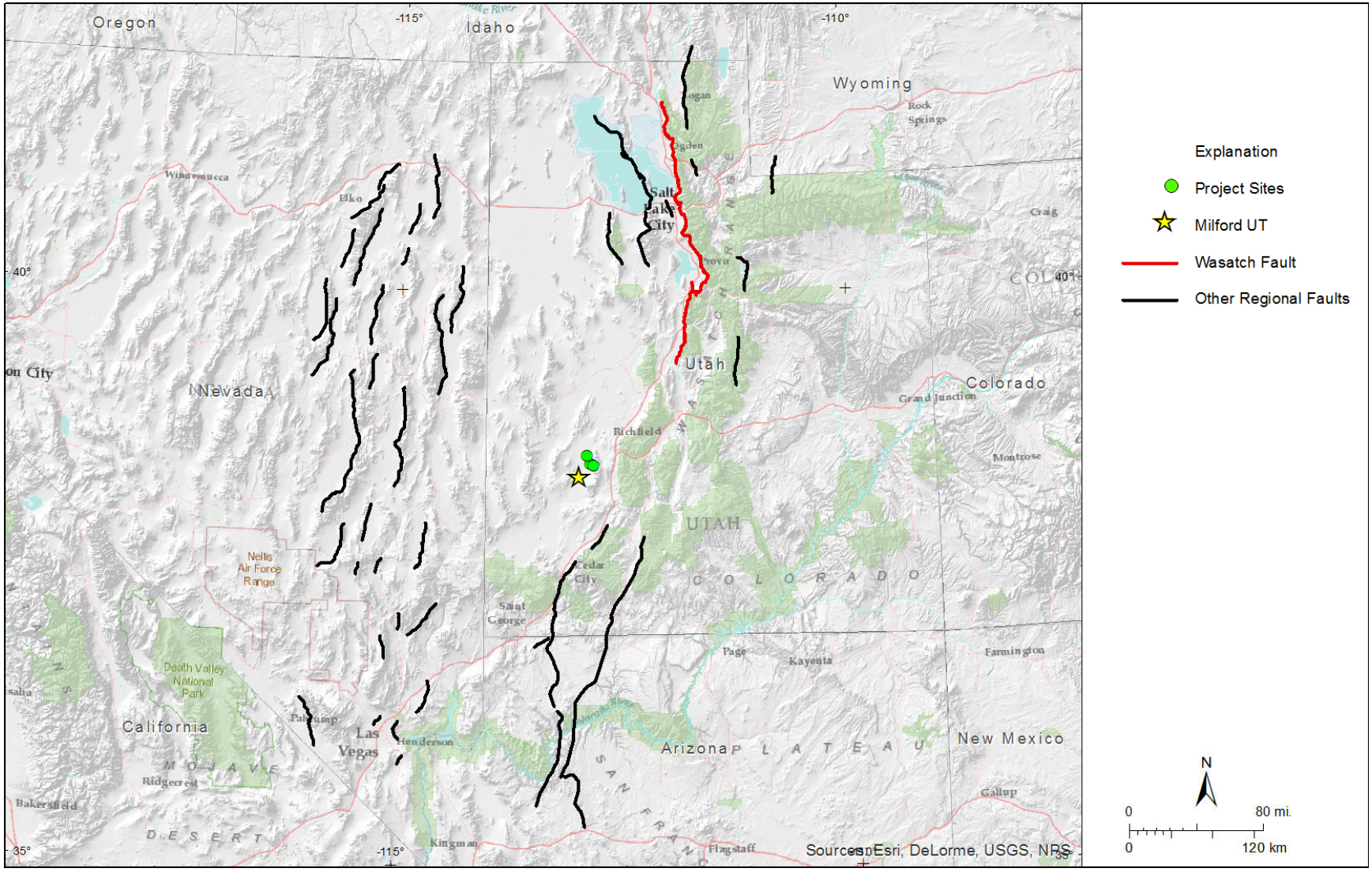

Figure 3-3: Regional Faults

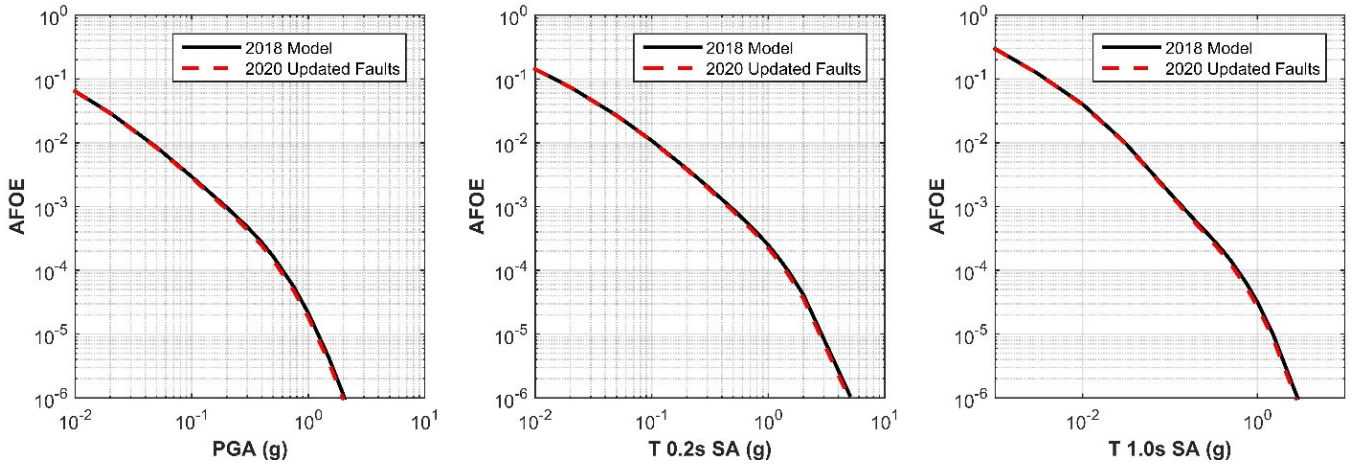

Figure 4-1: Effect of Updates in the Characterization of the Negromag and Wasatch Fault on the Seismic Hazard at the FORGE Drilling Center

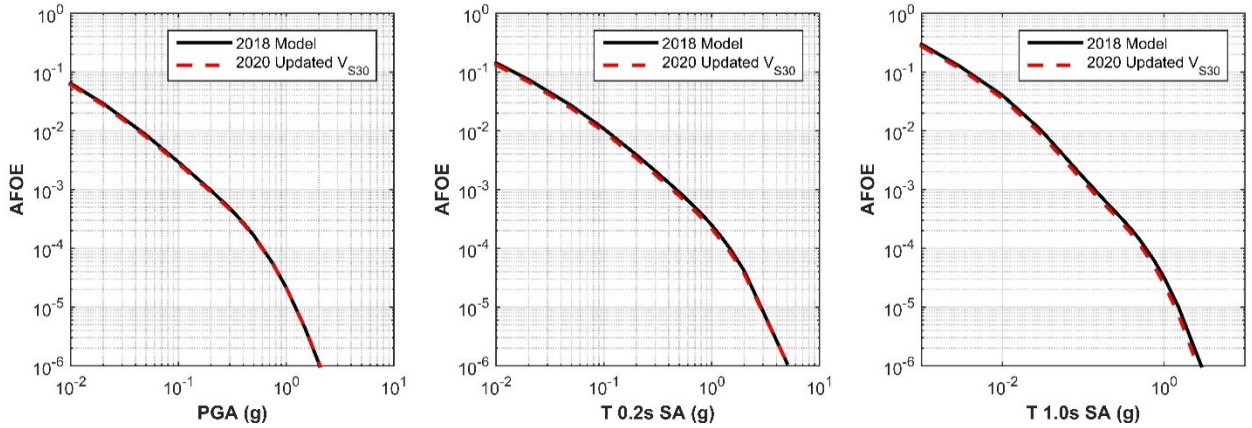

Figure 4-2: Effect of the updated site-specific adjustment of the NGA-West 2 models

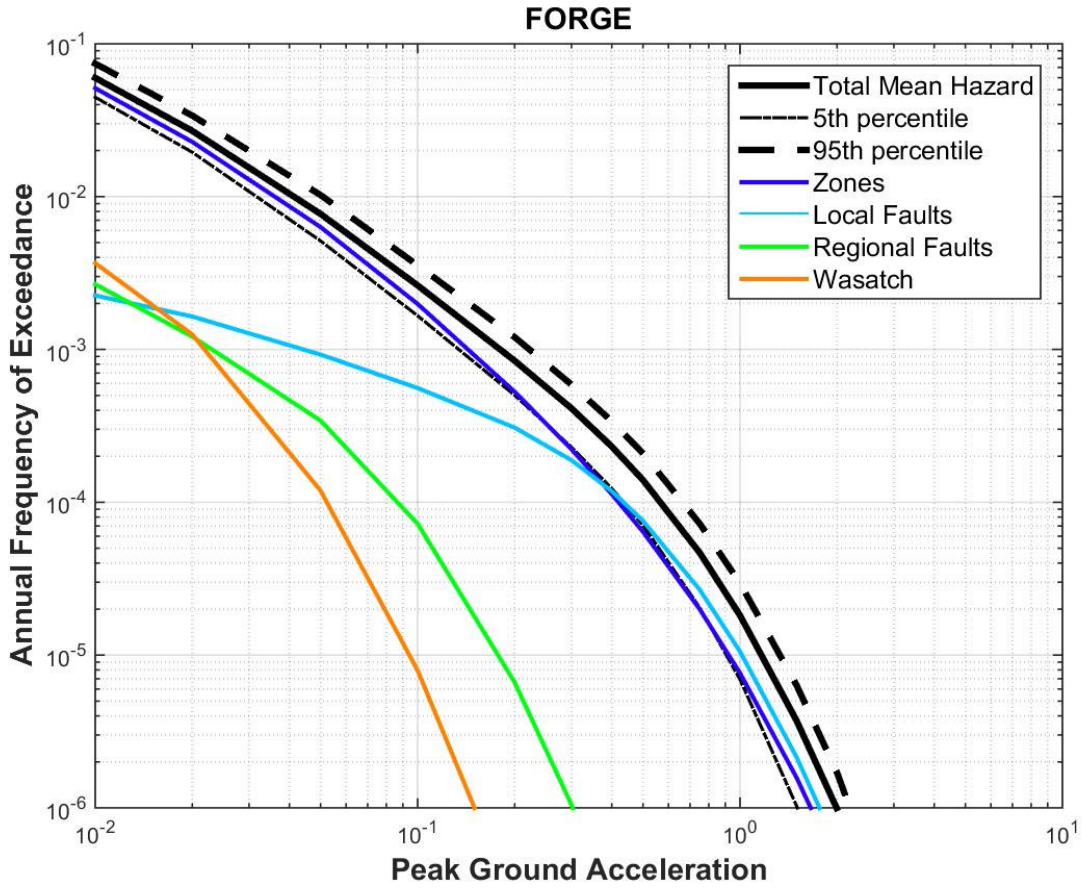

Figure 4-3: Total Mean Hazard for PGA and Grouped Source Contribution for the FORGE Drilling Center

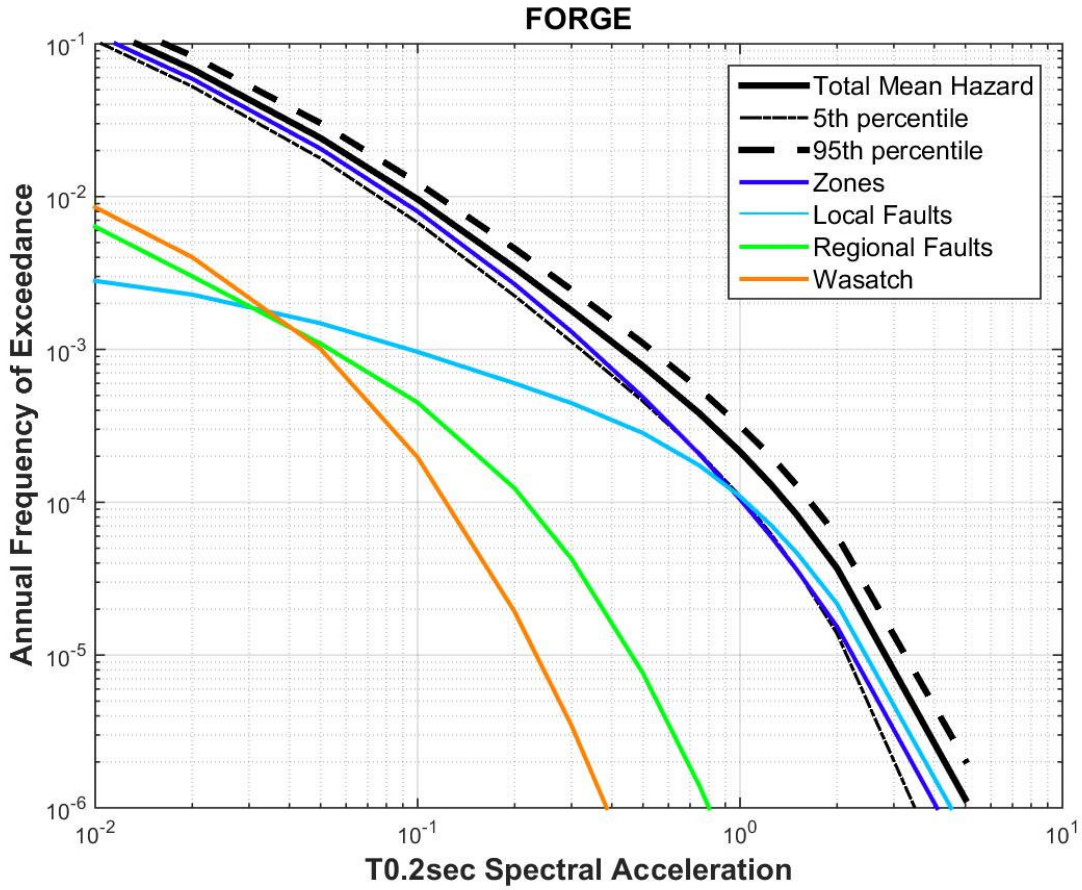

Figure 4-4: Total Mean Hazard for 0.2 s Spectral Acceleration and Grouped Source Contribution for the FORGE Drilling Center

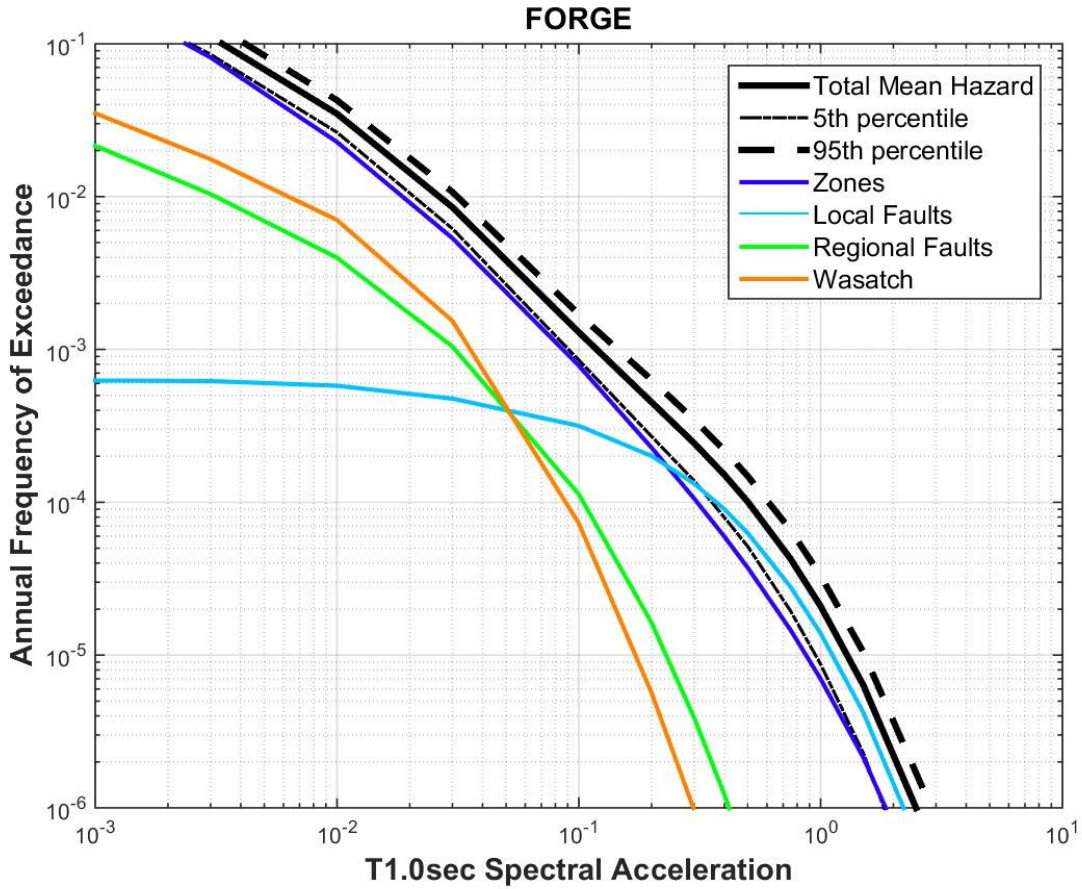

Figure 4-5: Total Mean Hazard for 1 s Spectral Acceleration and Grouped Source Contribution for the FORGE Drilling Center

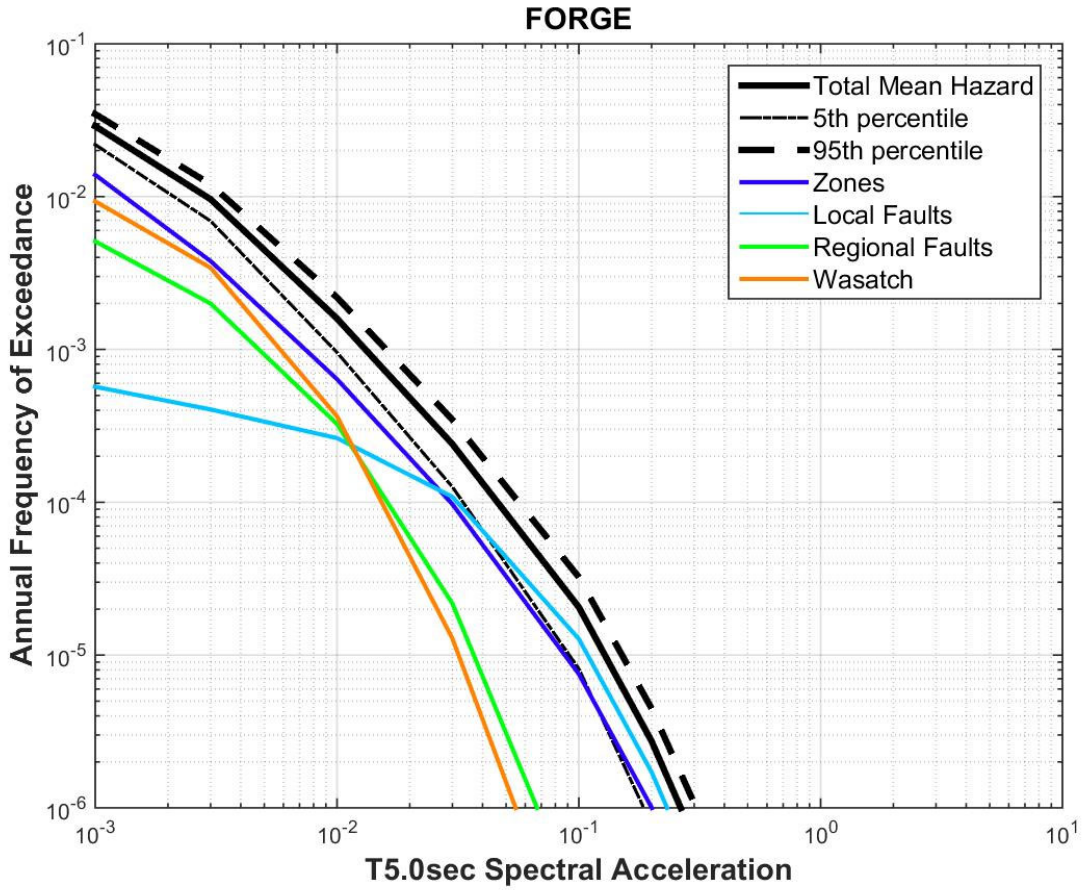

Figure 4-6: Total Mean Hazard for 5 s Spectral Acceleration and Grouped Source Contribution for the FORGE Drilling Center

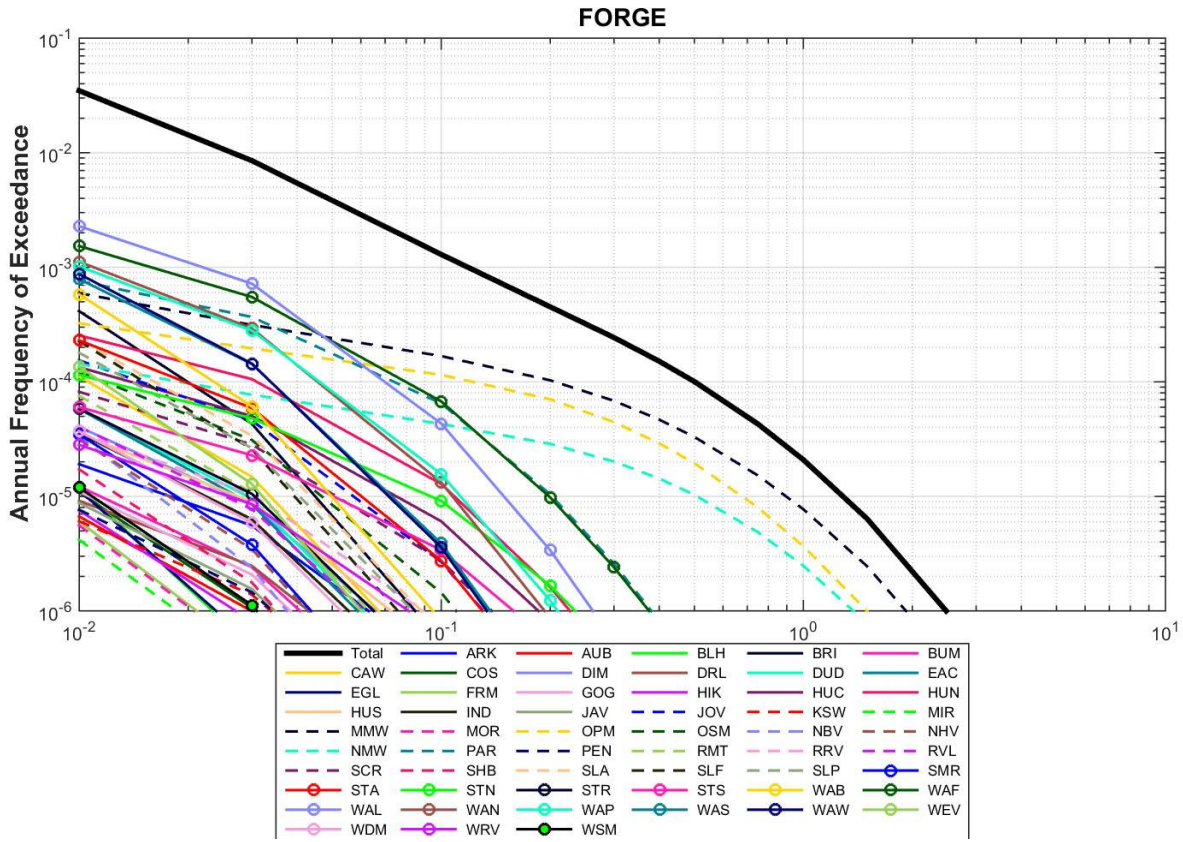

Figure 4-7: Seismic Hazard Curves for Local and Regional Faults for 1 s Spectral Acceleration at the FORGE Drilling Center

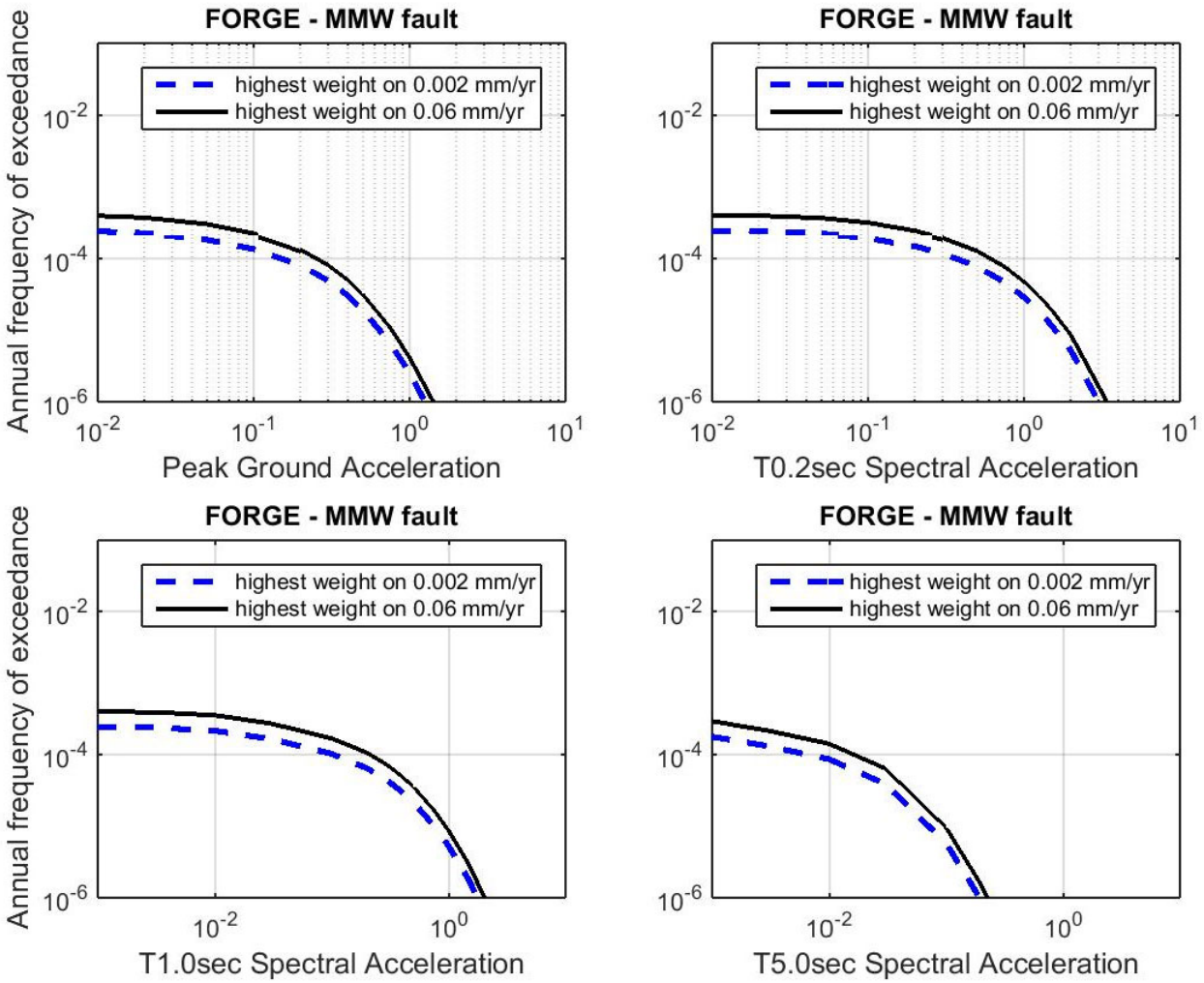

Figure 4-8: Sensitivity of the Mineral Mountain West Fault Hazard Curves to Changes in the Mean Slip Rate

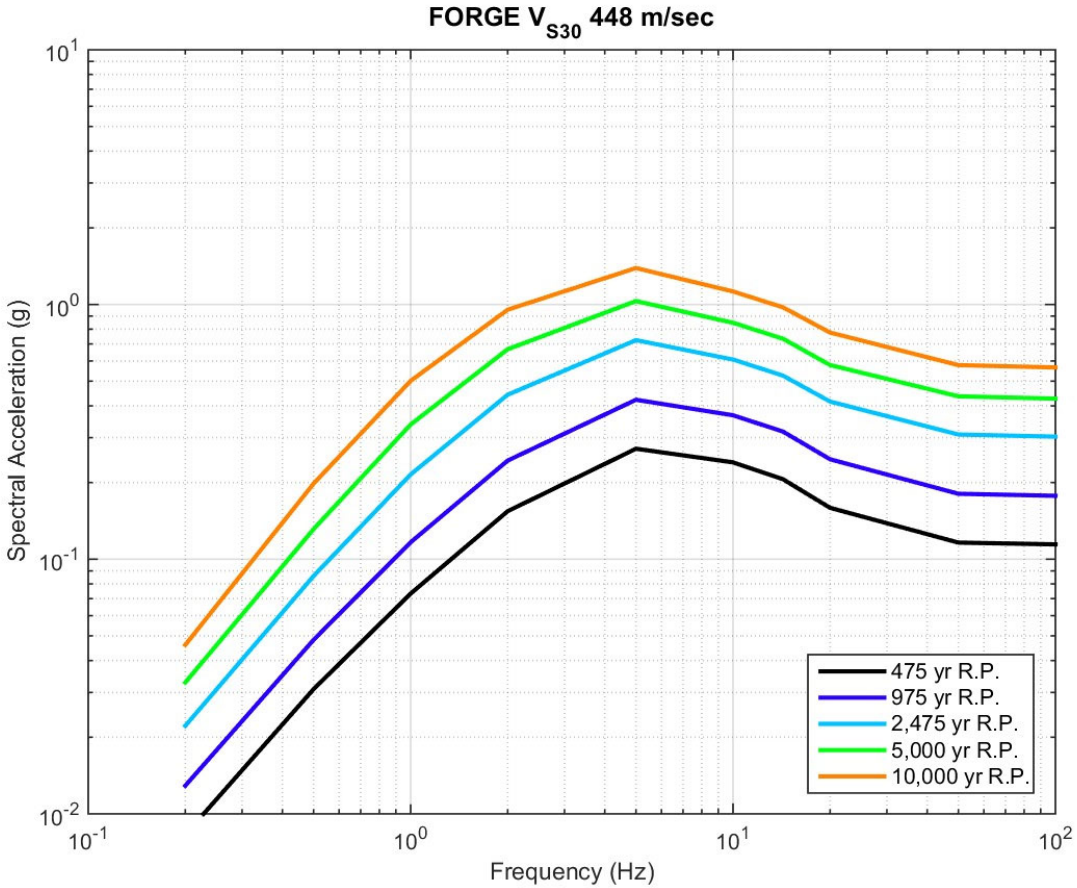

Figure 4-9: Mean Horizontal Uniform Hazard Response Spectra for the FORGE drilling Center

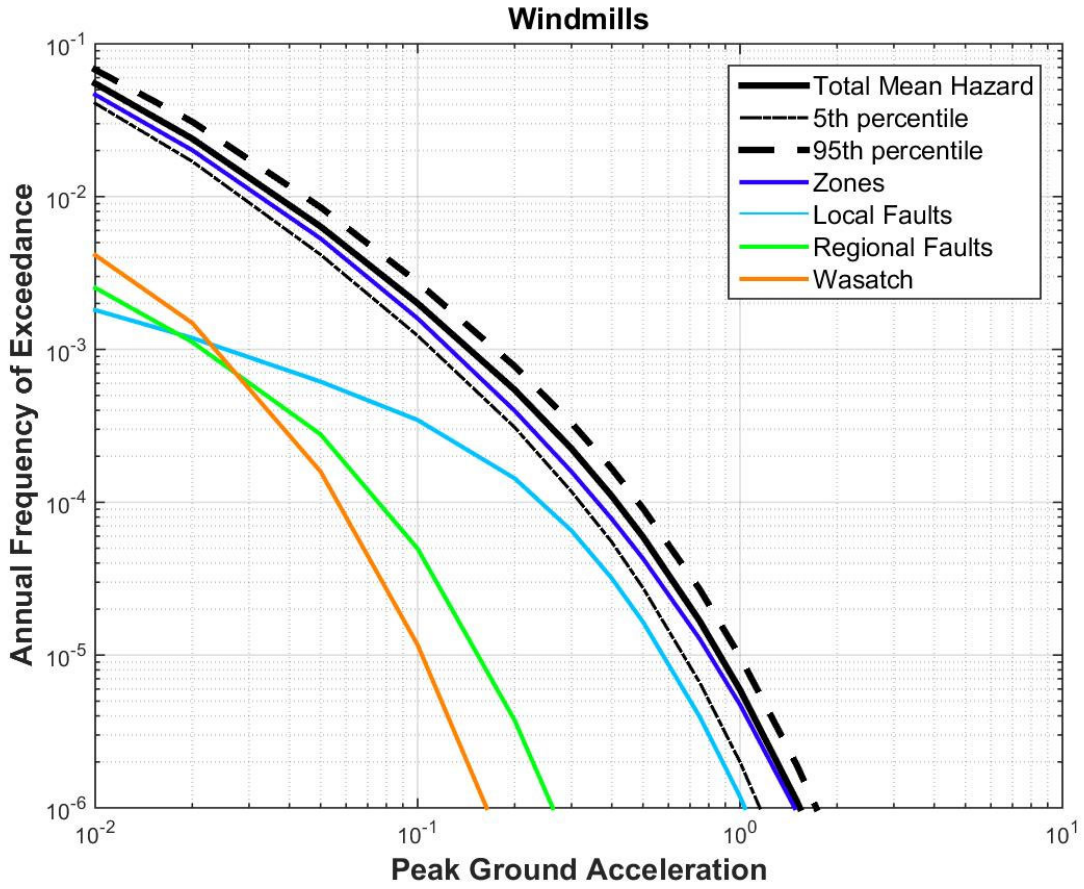

Figure 4-10: Total Mean Hazard for PGA and Grouped Source Contribution for the Windmills

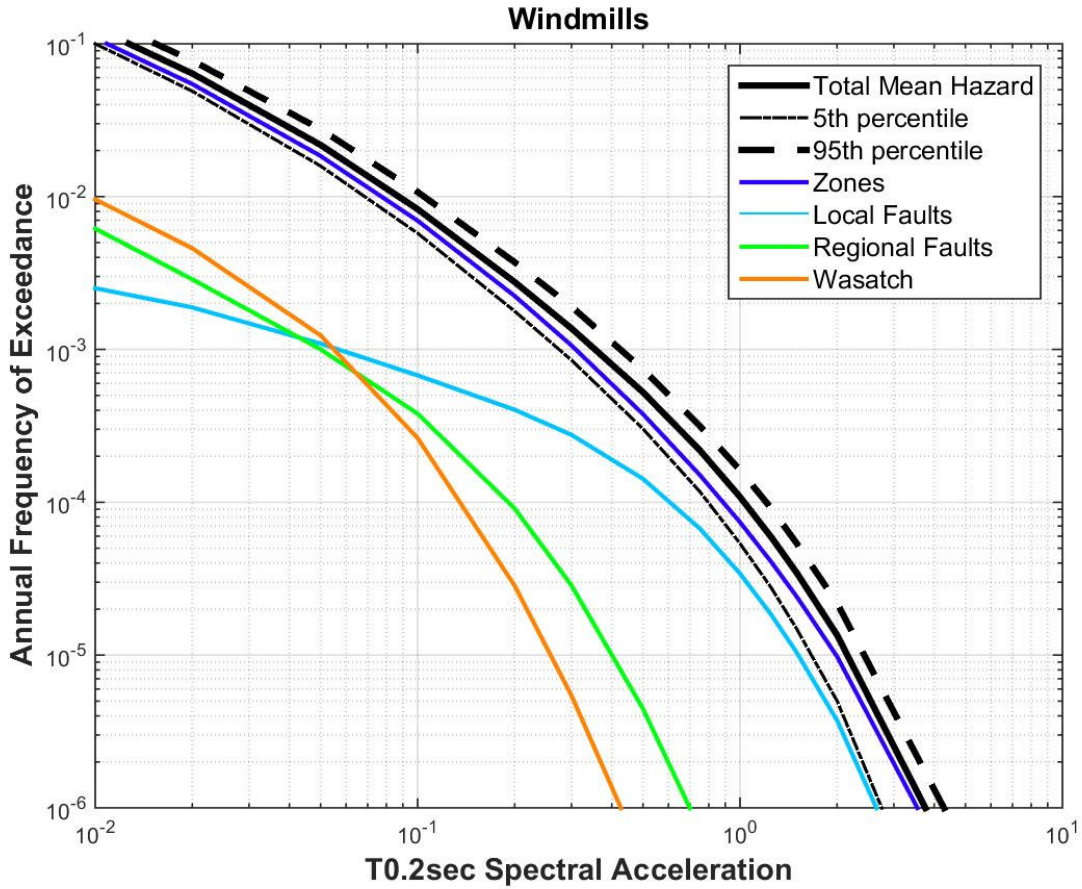

Figure 4-11: Total mean Hazard for 0.2 s Spectral Acceleration and Grouped Source Contribution for the Windmills

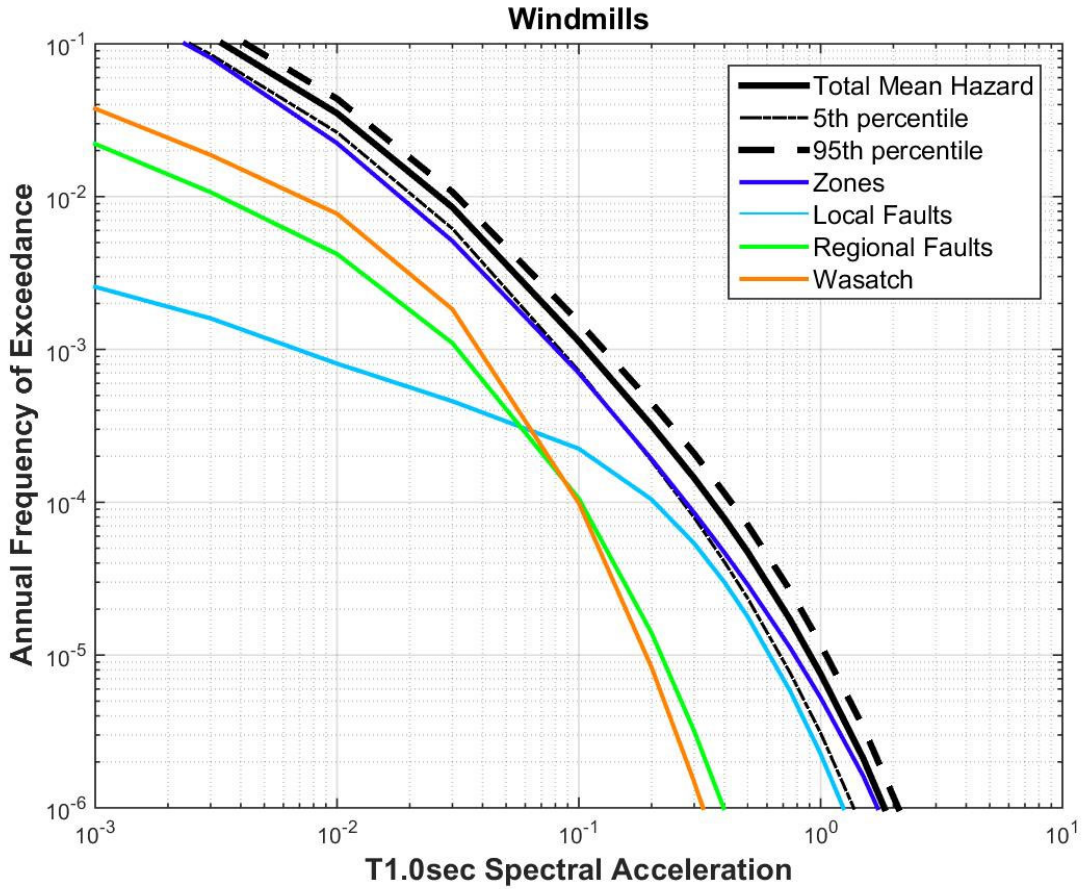

Figure 4-12: Total Mean Hazard for 1 s Spectral Acceleration and Grouped Source Contribution for the Windmills

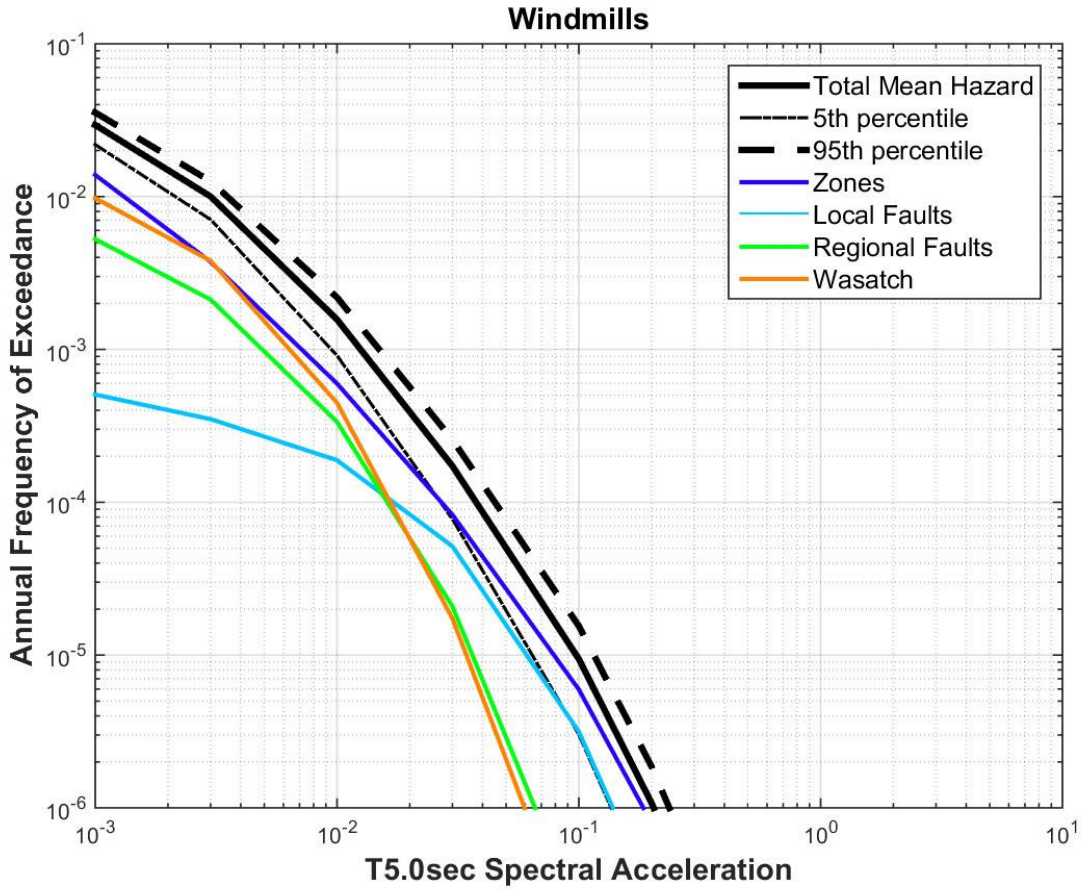

Figure 4-13: Total Mean Hazard for 5 s Spectral Acceleration and Grouped Source Contribution for the Windmills

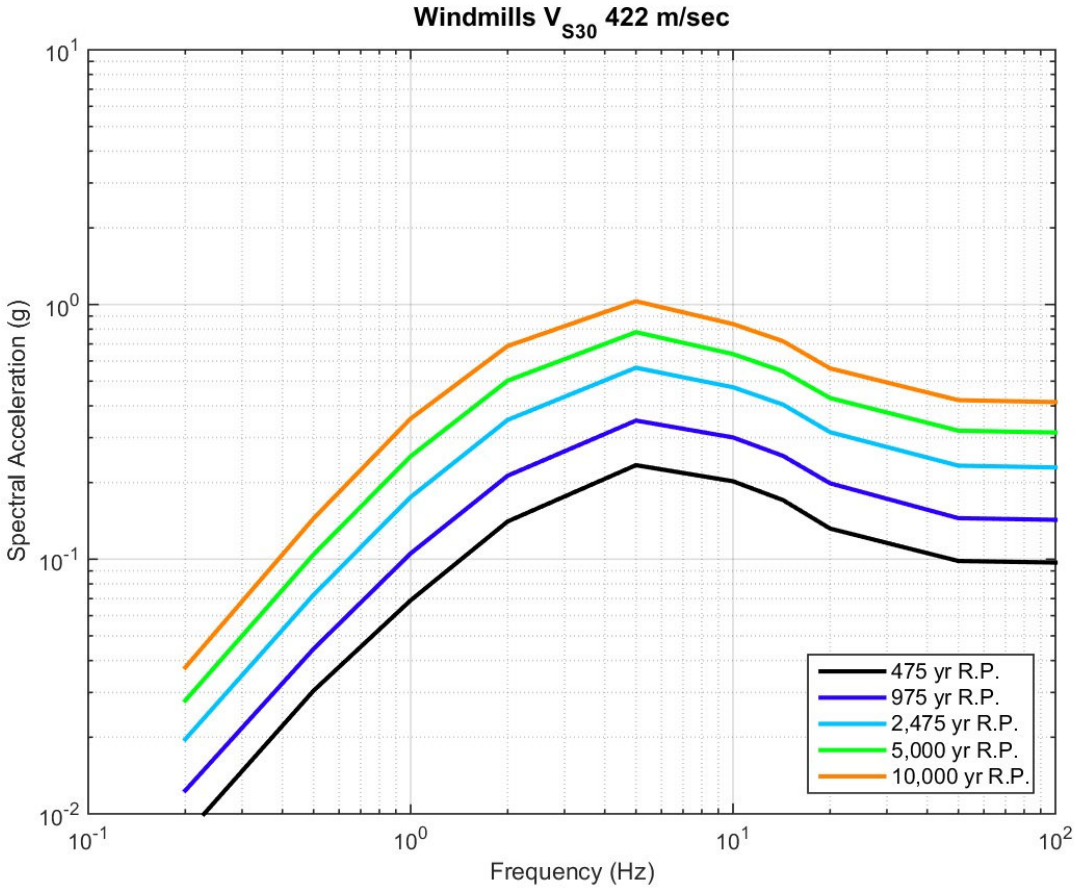

Figure 4-14: Mean Horizontal Uniform Hazard Response Spectra for the Windmills

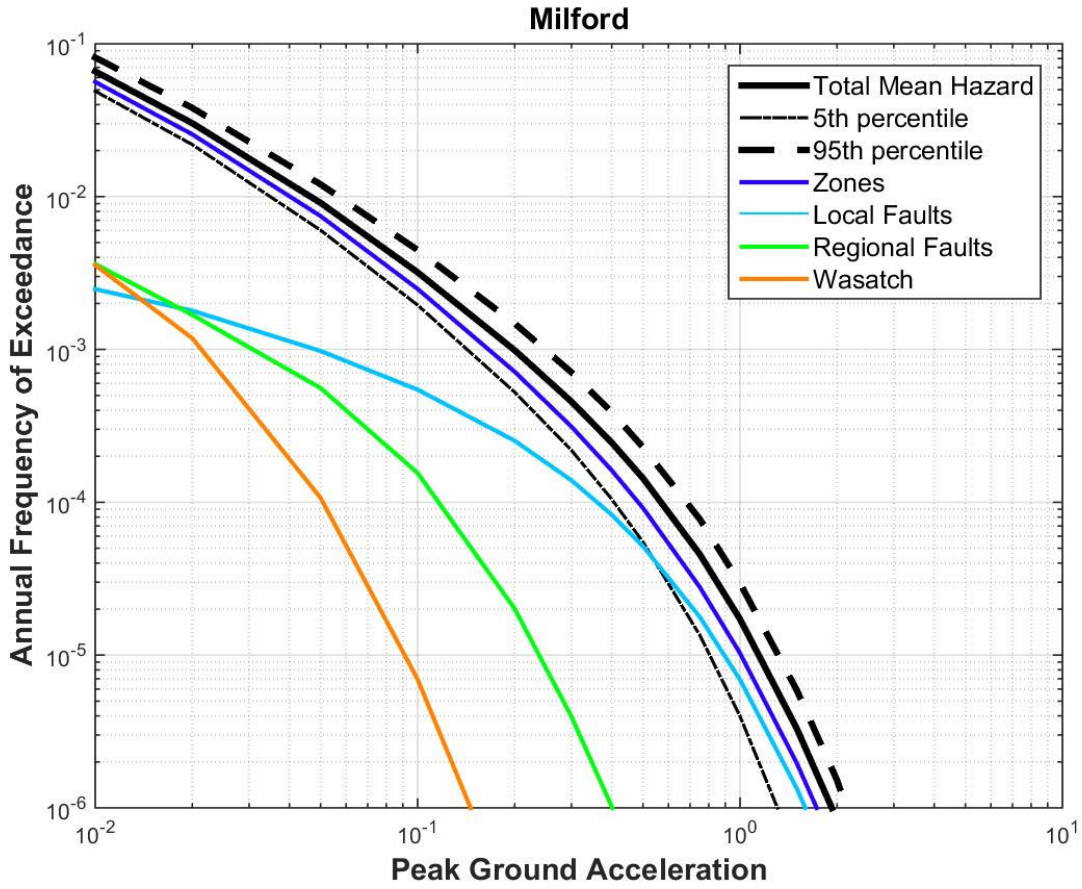

Figure 4-15: Total Mean Hazard for PGA and Grouped Source Contribution for Milford, UT

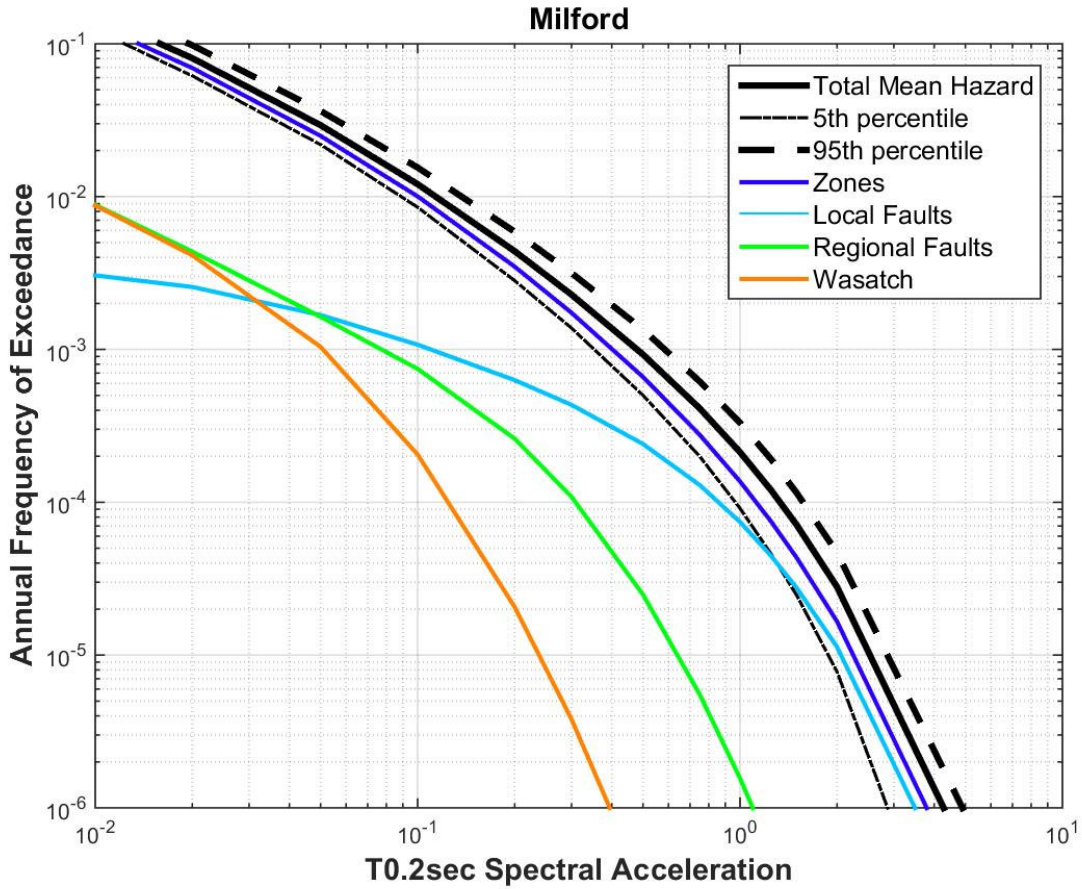

Figure 4-16: Total Mean Hazard for 0.2 s Spectral Acceleration and Grouped Source Contribution for Milford, UT

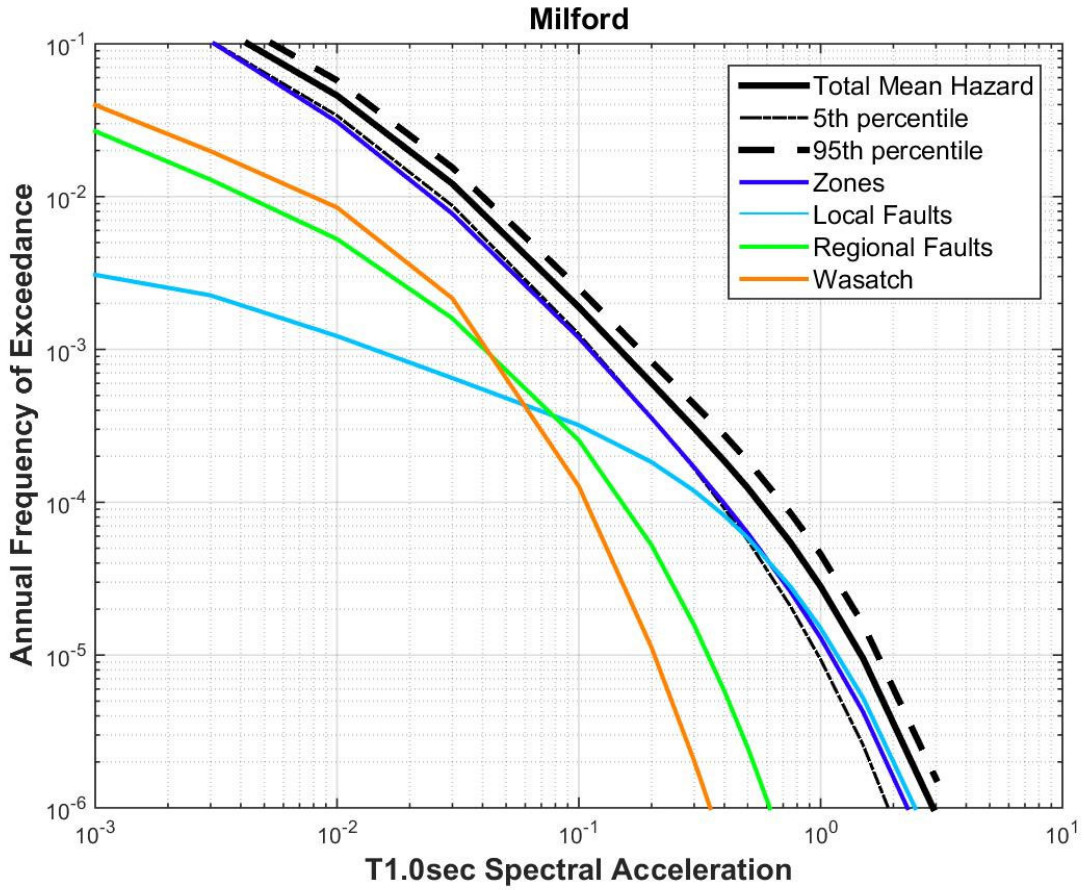

Figure 4-17: Total Mean Hazard for 1 s Spectral Acceleration and Grouped Source Contribution for Milford, UT

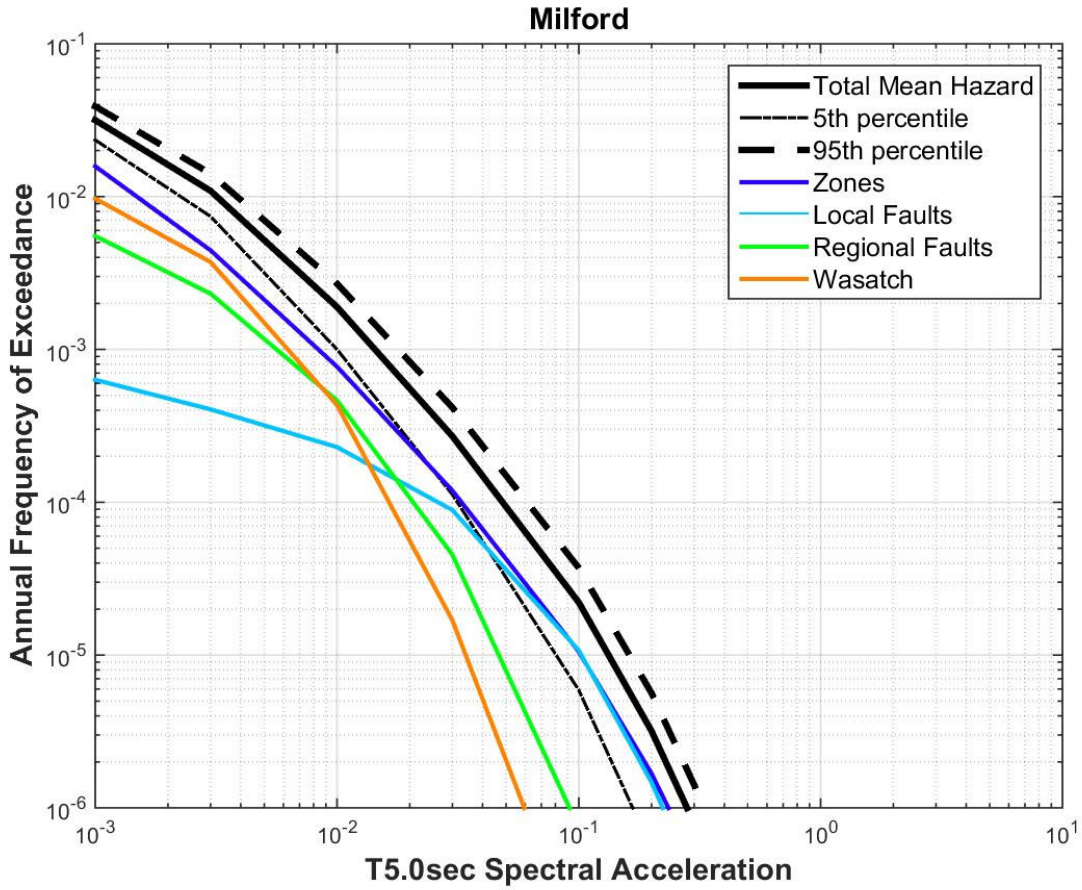

Figure 4-18: Total Mean Hazard for 5 s Spectral Acceleration and Grouped Source Contribution for Milford, UT

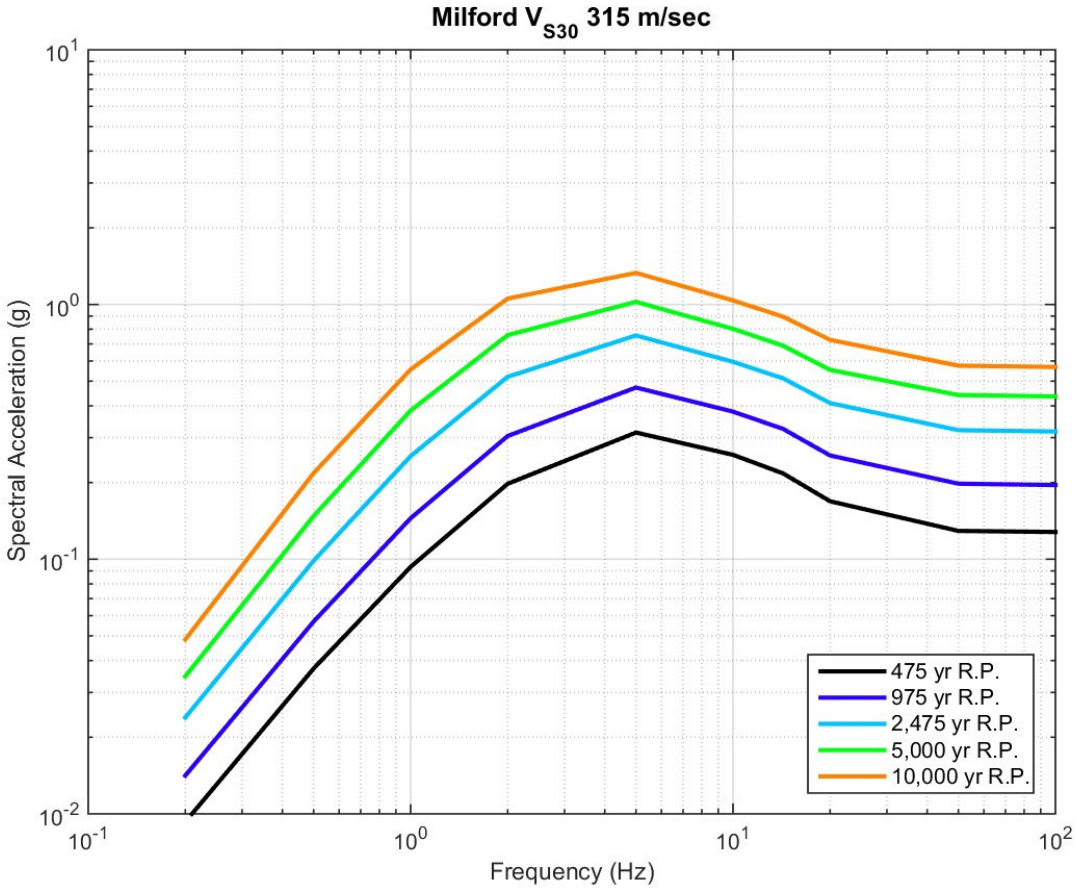

Figure 4-19: Mean Horizontal Uniform Hazard Response Spectra for Milford, UT

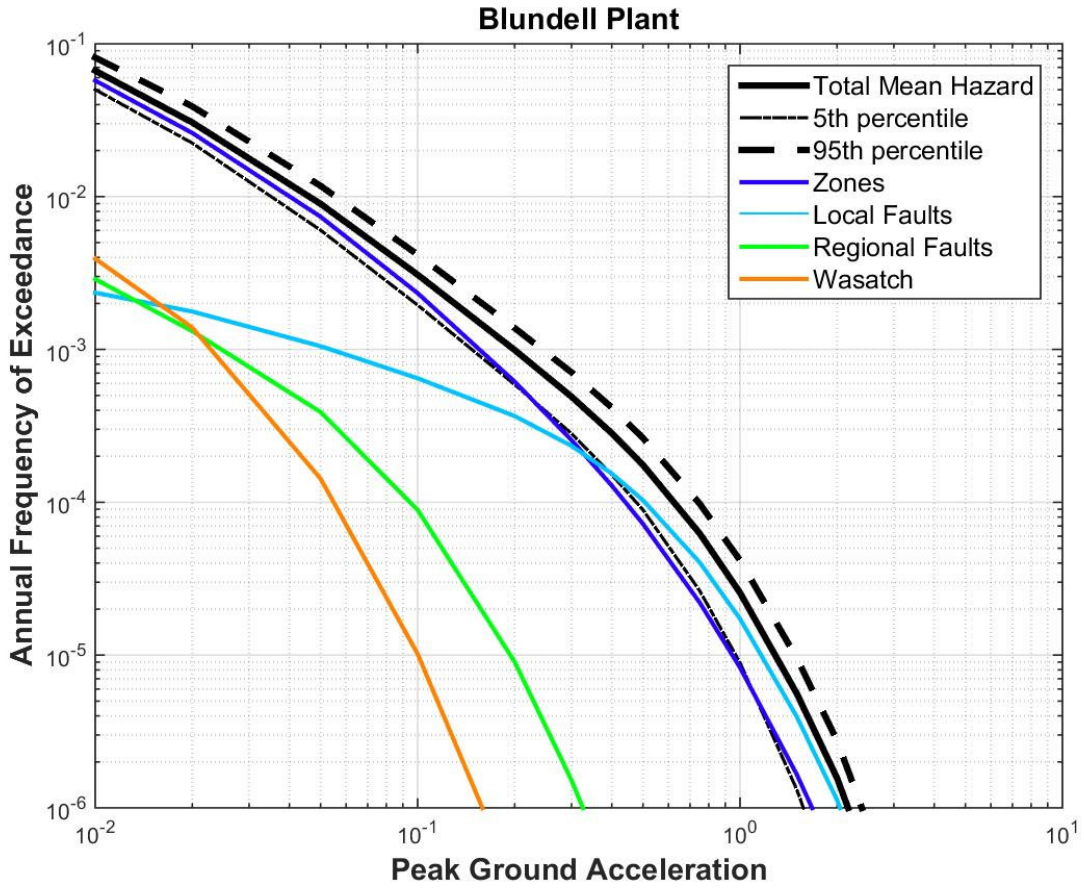

Figure 4-20: Total Mean Hazard for PGA and Grouped Source Contribution for the Blundell Geothermal Plant

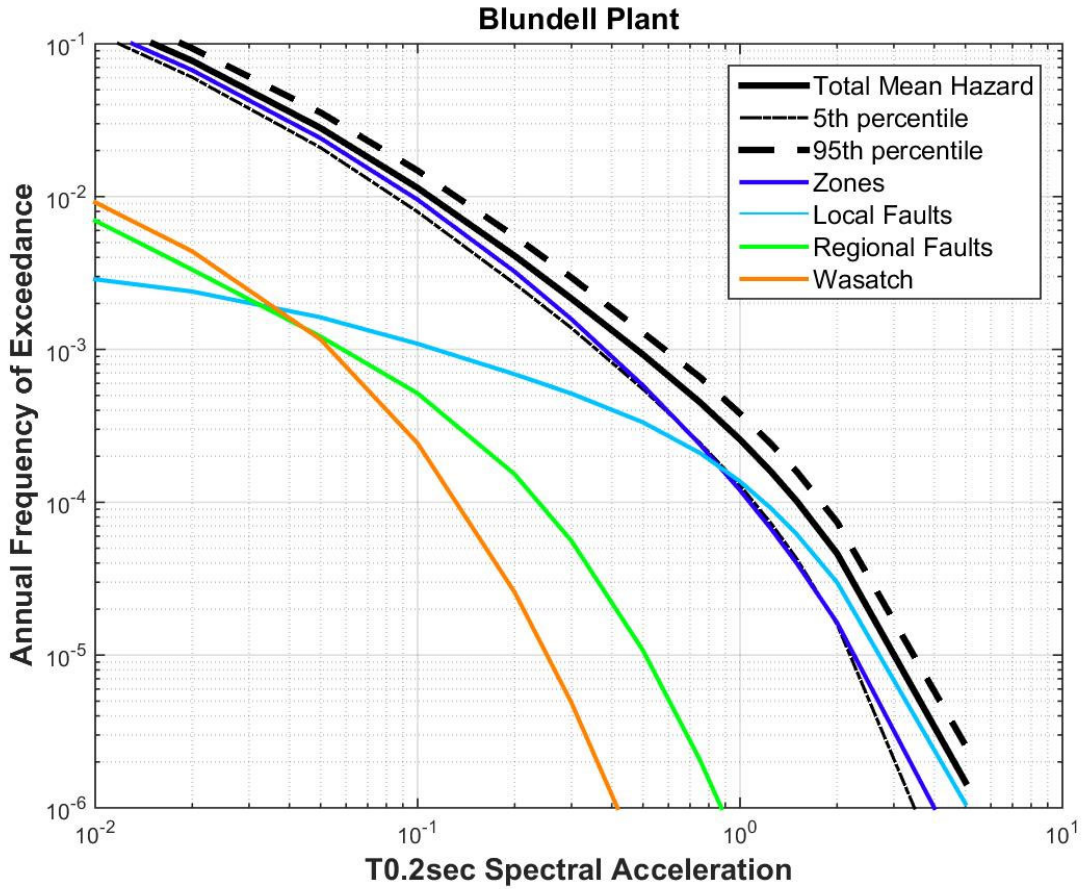

Figure 4-21: Total Mean Hazard for 0.2 s Spectral Acceleration and Grouped Source Contribution for the Blundell Geothermal Plant

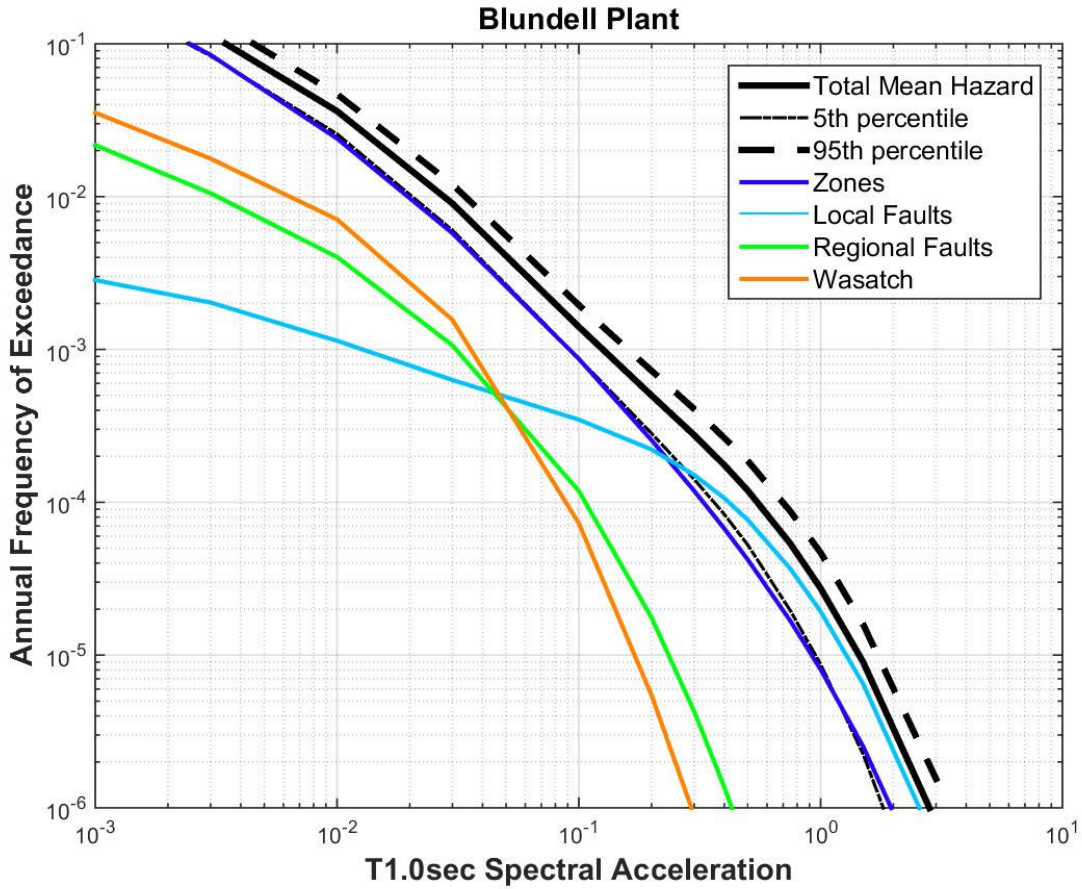

Figure 4-22: Total Mean Hazard for 1 s Spectral Acceleration and Grouped Source Contribution for the Blundell Geothermal Plant

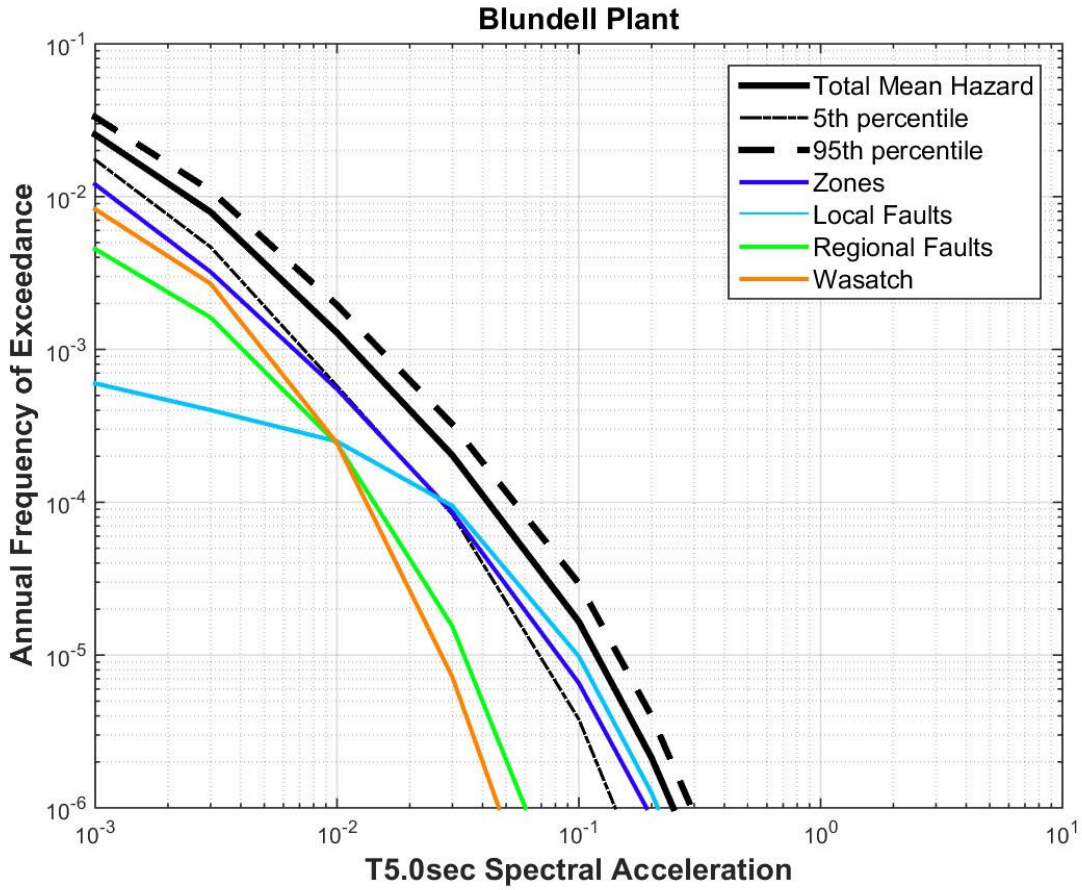

Figure 4-23: Total Mean Hazard for 5 s Spectral Acceleration and Grouped Source Contribution for the Blundell Geothermal Plant

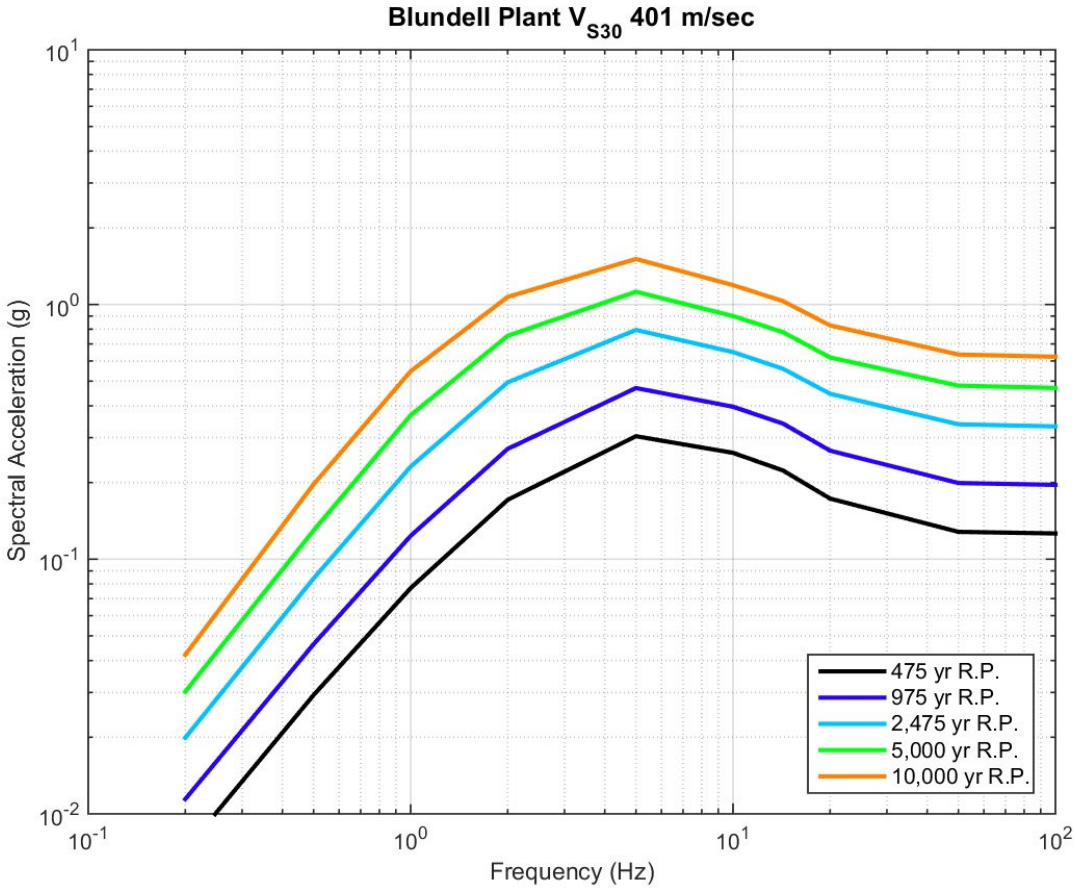

Figure 4-24: Mean Horizontal Uniform Hazard Response Spectra for the Blundell Geothermal Plant

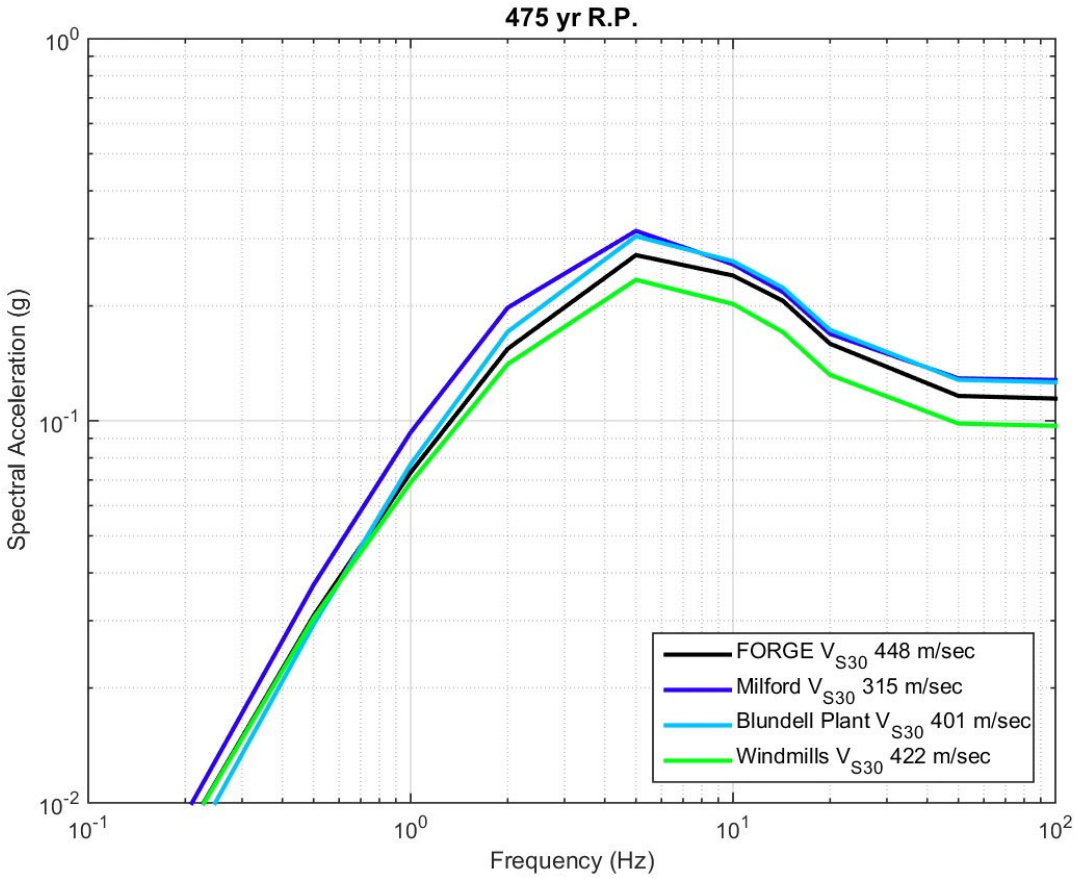

Figure 4-25: Comparison of the 475 Years Return Period Uniform Hazard Response Spectra for the Four Sites